Development of a Biaxial Stretch Bioreactor and Finite Element Models for Mechanobiological Study of Aortic Valve Leaflets

A Dissertation Presented for the
Doctor of Philosophy
Degree
The University of Tennessee, Knoxville

Ying Lei
December 2017

ACKNOWLEDGEMENTS

This work would not have been possible without Dr. Zannatul Ferdous' guidance and the financial support of the National Science Foundation as well as the Mechanical, Aerospace and Biomedical Engineering Department of the University of Tennessee, Knoxville. I am especially indebted to Dr. Anming Hu, Dr. Nicole McFarlane, Dr. Jeffrey A. Reinbolt and Dr. Jayne Wu, who supported me significantly when I experienced difficulties during my PhD program, and worked actively to provide me with advices to pursue the goals in my research plan. I am grateful to all of my colleagues and friends, with whom I experienced so much pleasure during and after the work. I would like to thank my parents and my husband, Hang Li, since they always tried to comfort me when I had to face anxiety, and never gave me any pressure on my process of completing the degree requirements.

ABSTRACT

Aortic heart valve disease is a significant cause of mortality worldwide; and replacement surgery is necessary in 70% of cases. Tissue engineered heart valves (TEHVs) are biocompatible and biodegradable, with ability to grow with the patient. However, to date, TEHVs mostly lack ability to withstand native mechanical forces since they are unable to mimic the heterogeneous and anisotropic structure of extracellular matrix (ECM) in native valves. Cyclic stretch is known to modulate ECM fiber synthesis and alignment. However, little tools are available for studying the interaction between aortic tissues and stretch condition. Finite element method is a powerful tool to simulate the complex structure of aortic valve, however, most current simulations modeled the leaflet as a homogenous material, and none of them took the distinctions between two surface layers into account, which were critical for the proper function of the aortic valve.

To study the effects of cyclic stretch on extracellular matrix remodeling, the heterogeneous properties of the aortic leaflet, and the effects of heterogeneity on the function of valve, we have 1) Designed, fabricated and validated a biaxial stretch bioreactor; 2) Analyzed train patterns of native aortic leaflets using digital image correlation method; 3) Designed and validated an anisotropic and heterogeneous finite element (FE) model for leaflets. These studies provided insights into the interaction between aortic valve tissue and the mechanical environment, anisotropy and heterogeneity of aortic leaflets ECM due to the

distribution of collagen fibers, and detailed distinct strain patterns in fibrosa vs. ventricularis sides and 3 aortic leaflets. Our novel biaxial stretch bioreactor and refined FE model of aortic leaflet will pave path for other scientists to study mechanobiology, design and condition engineered tissues and simulate engineered aortic valve grafts or pathology of calcium deposition.

TABLE OF CONTENTS

INTRODUCTION 1
CHAPTER I Design Considerations and Challenges for Mechanical Stretch Bioreactors in Tissue Engineering 10
- Abstract 11
- Introduction 12
- Design of stretch bioreactors 15
  - Actuating and motion transforming system 16
  - Monitoring and control system 20
  - Culture chambers 22
  - Nutrition exchanging system 24
  - Stretch regimen 24
- Tissue-engineered scaffolds for stretch bioreactors 25
  - Decellularized tissue scaffolds 27
  - Biomaterial scaffolds 28
  - Biodegradable polymer scaffolds 29
  - Techniques to generate anisotropic engineered tissues 30
- Conclusions and future directions 33
- References 36
- Appendix 48

CHAPTER II A Study of Extracellular Matrix Remodeling in Aortic Heart Valves Using a Novel Biaxial Stretch Bioreactor 53
- Abstract 54
- Introduction 55
- Materials and Methods 58
  - Design and fabrication of the bioreactor 58
  - Digital image correlation analysis 60
  - Validation of controlled biaxial stretch 61
  - Measuring strain patterns of coronary and noncoronary cusps 61
  - Cyclic stretch conditioning 62
  - Hematoxylin & Eosin (H&E) staining, DNA, collagen and GAG assays 63
  - Maintenance of sterility 64
  - Statistical Analysis 64
- Results 64
  - DIC results on silicone rubber membrane 64
  - Finite element analysis 65
  - Strain fields on fresh aortic valve cusps 65
  - Strain fields on stretched cusps and controls 66
  - Collagen and GAG contents in stretched cusps and controls 66
- Discussion 67
  - Validation of the stretch 68
  - Biaxial stretch improved maintenance of native ECM structure 69
  - Distinct strain patterns of fresh aortic valve cusps 70

Limitations and future works....72
Conclusions....73
Acknowledgements....74
References....75
Appendix....81
CHAPTER III A layered and heterogeneous finite element model for mechanobiologicalsimulation of aortic valves....88
Abstract....89
Introduction and literature review....90
Application of finite element method in aortic valve study....90
Difficulties in simulation of aortic valves....93
Method....98
Geometric model....99
Hyperelastic material models....102
Results and Discussion....104
Conclusion....107
References....108
Appendix....112
CONCLUSION....117
VITA....119

LIST OF FIGURES

Figure 1. Location of the aortic valve 1
Figure 2. Healthy vs. diseased aortic valves 2
Figure 3. Three layered structure of a leaflet 4
Figure 4. Collagen fibers in a leaflet 4
Figure 5. Testing strain field of a tendon using DIC meth 7
Figure 6. Loading condition and deformation of a membrane 7
Figure 7. Different actuating units for stretch bioreactors: 51
Figure 8. Different Transforming units for linear motions: 52
Figure 9. Layout of the custom biaxial stretch bioreactor. 81
Figure 10. Radial, circumferential and shear strain 82
Figure 11. Strain pattern on a leaflet 83
Figure 12. Strain patterns on two sides of a leaflet 83
Figure 13. Strain patterns on leaflets of one valve 84
Figure 14. Strain patterns showed by average strain 85
Figure 15. Results of experimental and control groups 86
Figure 16. H&E straining of experimental and control groups 87
Figure 17. Polarized light image and major fiber bundles of a leaflet 112
Figure 18. Stress-strain relationships 112
Figure 19. Experimental data on two sides of leaflets 113
Figure 20. Elastic base was meshed with 3D elements 113
Figure 21. Collagen fibers were meshed with 1D elements 114
Figure 22. Curve fitted stress-strain relationships under uniaxial stretch 115
Figure 23. Strain patterns generated by simulation 115
Figure 24. Validation of strain patterns 116
Figure 25. Constitutive model under equibiaxial stretch 116

INTRODUCTION

Heart valves facilitate the circulation of blood. During systole, the aortic valve opens to allow the blood to be pumped out of the heart; while during diastole, it closes to prevent the backflow to the left ventricle where the pressure is lower. It opens and closes 100,000 times every day amounting to around 3 billion cycles over the life-time of an average adult. Aortic valve disease occurs when heart valves are unable to fully open, impeding blood flow, or are unable to fully close, causing blood to flow backwards.

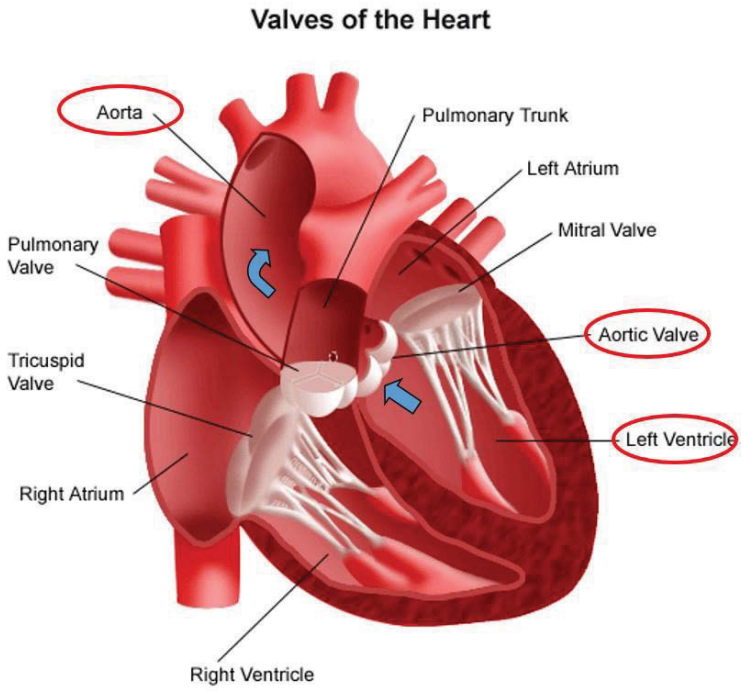


Figure 1. Location of the aortic valve

In the United States alone, as the American Heart Association reported, the overall prevalence of VHD in 2005 was about 1.8% which means around 5.2 million people suffered from it. In particular, congenital heart valve defects affect 1-2% of all live births which can be fatal if left untreated. In addition, among people over 65 years old, the prevalence increases to 10.7% which indicates it is an age-related process caused by the repetitive mechanical stimuli on valves across the lifespan.

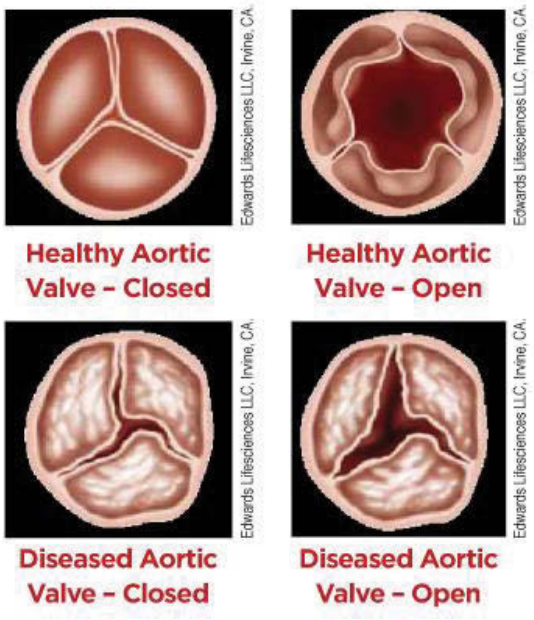


Figure 2. Healthy vs. diseased aortic valves

Although repair and preservation of diseased valves is preferable, in 70% of cases, extensive replacement is necessary. Replacement valves in current clinical use fall into two categories. Biological valves manufactured from decellularized heart valves have a limited expected lifespan of approximately 15 years. Mechanical prosthetic valves generally last longer but require lifelong anticoagulant treatment

due to their thrombogenic properties. Neither of these approaches meets the needs of children, who need the implants to grow with them. Tissue engineered heart valves have the potential to last longer and minimize immune response since they are autologous living tissues that can integrate, remodel and grow with the patient. However, they mostly lack ability to withstand native mechanical forces since they are unable to mimic the heterogeneous and anisotropic structure of extracellular matrix in native valves.

Aortic valves consist of three semicircular leaflets attached to a fibrous root. Valvular interstitial cells produce ECM to support the cells and bear the loads. The leaflets consist of three distinct layers: the fibrosa, spongiosa and ventricularis. Within the fibrosa, the primary tensile load-bearing layer, collagen fibers are highly aligned in the circumferential direction, resulting in tissue anisotropy**.** It has been found that the fibrosa is 4-6 times stiffer in the circumferential direction. In addition to circumferentially oriented collagen, the largest and strongest collagen fiber bundles are localized in the areas of greatest tensile stress along the lower part of the commissure and coapting regions. This particular architecture of collagen fibers contributes to the heterogeneous mechanical behavior of the aortic valve leaflet. Since cyclic stretch is known to modulate cells differentiation, ECM synthesis and organization, understanding the interactions between stretch, cells and ECM will not only facilitate the design of functional TEHVs, but also will provide insight on valve biology and pathology.

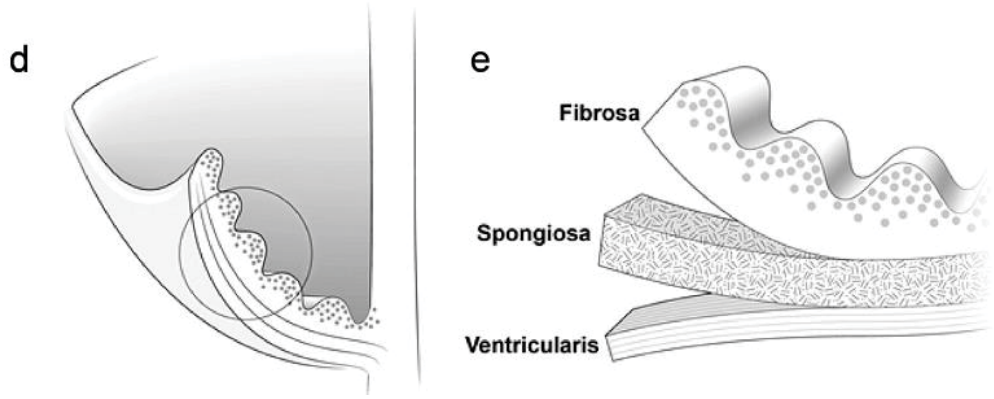


Figure 3. Three layered structure of a leaflet



Figure 4. Collagen fibers in a leaflet

Aortic valves experience unique bidirectional stretch in vivo, where the cusps encounter approximately 13–25% strain in the radial direction and 10% strain in the circumferential direction. This physiological strain profile is critical for regulating the cell turnover and alignment in healthy aortic valves. It also guides extracellular matrix (ECM) fibers to be organized in radial and circumferential directions within the cusps, which is necessary for the proper coaptation of valves. On the other

hand, pathological stretch condition causes elevated cell proliferation and apoptosis rate, increased proteolytic enzyme activities, and calcifications in diseased aortic valves.

To mimic these stretch conditions in a tissue culture environment, a variety of uniaxial and biaxial stretch bioreactors have been used for tissue engineering and mechanobiology studies of aortic valves. Effects of uniaxial stretch has been extensively studied, alone or in combination with other mechanical stimuli such as flexure, flow-based shear stress or pressure. While biaxial stretch best mimics the stretch environment of aortic valves, the majority of these biaxial devices are designed to apply equibiaxial cyclic stretch. Recently reported bioreactors applied anisotropic strain profile to valvular cell-seeded engineered tissues by modifying the shape of collagen gels (circular vs. ellipsoidal, major/minor axis ratios 1:1, 2:1, and 4:1) cultured under equibiaxial strain. The control on the strain amount in these studies depended on the dimension (major/minor axis ratio) of the substrate. Alternatively, a cross-shaped mold was used to create collagen gels containing dermal fibroblasts, and the two axes/arms were subjected to different amounts of stretch. This resulted in uniaxial strain in the arms and anisotropic biaxial strain in the central region (overlap of the two arms) of the cross-shaped tissue.

Strain fields help to elucidate the anisotropic and heterogeneous mechanical properties of heart valves. Previous studies have tested the stress-strain curve of

healthy aortic cusps cultured under uniaxial stretch, and built their general deformation models during systole and diastole *in vivo* based on ultrasound and computed tomography techniques. Recent studies tracked the deformations of a set of markers on the leaflets during stretch *in vitro*, and suggested a distinct mechanical behavior on different sections (free edge, middle, and root area) of the aortic cusps. However, in terms of microstructure, detailed deformation and strain maps of the entire valve cusp under biaxial stretch still need to be determined using a novel method.

Digital image correlation (DIC) method is a powerful tool to evaluate the deformation of a sample by comparing changes in a marker field on an original sample vs. a deformed sample. Since it is based on the gray scale values of pixels in a digital image, DIC offers strain analysis with high precision compared to traditional methods. To accurately track the markers, the marker field needs to have a non-repetitive and high contrast pattern. Depending on the size of a sample, a paint spray or an airbrush are most commonly used to generate a random marker field.

Although existing bioreactors have advanced cardiovascular research tremendously, to the best of the author's knowledge, a culture system that can apply physiological biaxial cyclic stretch while providing detailed strain monitoring is absent, leaving a pressing demand of developing a bioreactor with utility in both

mechanobiology studies and tissue engineering applications. Therefore our bioreactor will provide a suitable conditioning system to study remolding and heterogeneity of ECM, facilitating the design of engineered tissues.

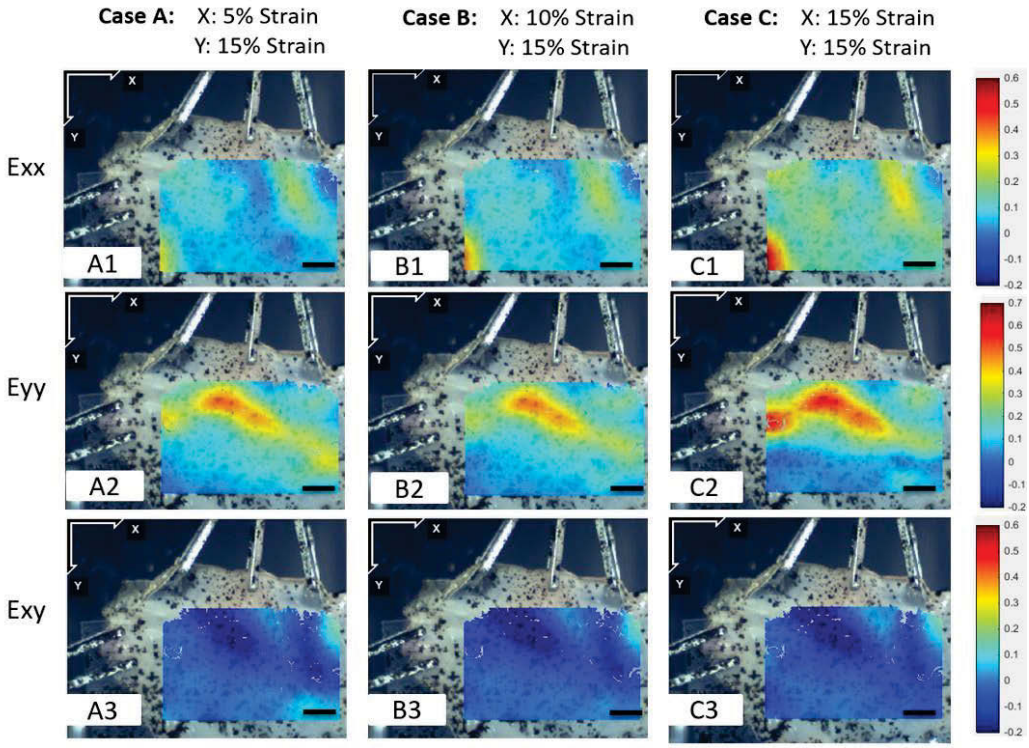


Figure 5. Testing strain field of a tendon using DIC meth

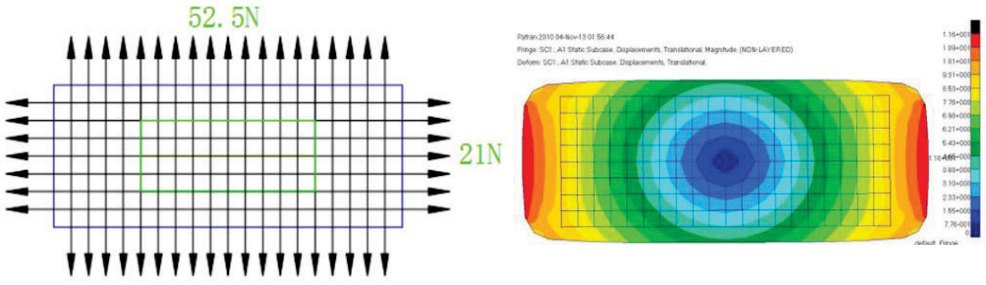


Figure 6. Loading condition and deformation of a membrane

Finite element method (FEM) is a powerful tool to study the mechanical behavior of heart valves due to its ability of greatly reducing the costs in setting up the experiments. In a typical process of finite element method, firstly the geometric model should be established to define the shape of the model. Then the model would be divided into discretized elements for calculation. The next step should be selecting the materials and applying their mechanical properties on the elements. After applying proper boundary conditions and loads, the deformation, stress and strain fields could be obtained finally. Due to the nonlinear stress-strain relationship of aortic valves, few numerical studies assumed linear elastic and isotropic or anisotropic tissue behavior. More advanced material models included nonlinear tissue behavior and constitutive models to account for their complex collagenous structure. However, current researches generally assume that the leaflet materials were homogeneous, treating them as composites with thin collagen fibers as reinforcement component embedded in elastic base materials. Since the thick collagen bundles on the fibrosa side were ignored using this method, some researchers improved the accuracy by including symmetric thick collagen network in their single layered models. However, our previous study showed that the fibrosa side was more heterogeneous and anisotropic than the ventricularis side, since the collagen fibers are mostly distributed on the fibrosa side. The fibers gather as thick bundles along circumferential direction, which move apart like springs during diastole to ensure large radial deformation. During systole, the cusps have a

relatively short elongation due to abundant elastin on the ventricularis side, which reduces the friction and resistance while the blood passes through it. We hypothesize that including the distinctions between fibrosa and ventricularis will improve the accuracy of the FE model. This refined model will facilitate simulation of fluid-structure interaction, calcium deposition, transcatheter aortic valve as well as design of implants for aortic valve replacement or repair.

CHAPTER I
DESIGN CONSIDERATIONS AND CHALLENGES FOR MECHANICAL STRETCH BIOREACTORS IN TISSUE ENGINEERING

A version of this chapter was originally published by Ying Lei and Zannatul Ferouds:

Ying Lei and Zannatul Ferdous. “Design Considerations and Challenges for Mechanical Stretch Bioreactors in Tissue Engineering.” *Biotechnology Progress*. 32(2016): 543-53.

Ying Lei was responsible for literature review, material collection, drafting and revision. Zannatul Ferdous was responsible for draft submission and revision.

Abstract

With the increase in life expectancy and growing aging population, lack of functional grafts for replacement surgeries has become a severe problem. Engineered tissues are a promising alternative to this problem because they can mimic the physiological function of the native tissues and be cultured on demand. Cyclic stretch is important for developing many engineered tissues such as hearts, heart valves, muscles, and bones. Thus a variety of stretch bioreactors and corresponding scaffolds have been designed and tested to study the underlying mechanism of tissue formation and to optimize the mechanical conditions applied to the engineered tissues.

In this review, we look at various designs of stretch bioreactors and common scaffolds are discussed and offer insights for future improvements in tissue engineering applications. First, the requirements and common configuration of stretch bioreactors are summarized. Next, the features of different actuating and motion transforming systems and their applications are presented. Since most bioreactors need to measure detailed distributions of loads and deformations on engineered tissues, techniques with high accuracy, precision and frequency have been developed. We also cover the key points in designing culture chambers, nutrition exchanging systems and regimens used for specific tissues. Since scaffolds are essential for providing biophysical microenvironments for residing cells, we discuss materials and technologies used in fabricating scaffolds to mimic anisotropic native tissues, including decellularized tissues, hydrogels, biocompatible polymers, electrospinning and 3D bioprinting techniques. Finally, we present the potential future directions for improving stretch bioreactors and scaffolds.

Key words: Tissue engineering; Cyclic stretch; Bioreactors; Scaffolds;

Introduction

Replacement surgery is often the primary option for patients with irreversibly damaged or failed organs and tissues.[1-4] However, with increased average life

expectancy and a growing aging population, there is a severe shortage of donor organs and tissues. According to the U.S. Department of Health & Human Services, the gap between people on the waiting list for a transplant and donor organs increased from 7,442 to 92,318 between 1991 and 2013; 122,407 people are currently waiting for an organ, while 22 on the waiting list are projected to die each day in 2015.[5] Furthermore, there are limitations associated with allografts or donor tissues, for example, host body rejection, disease transmission, size mismatching, etc.[6] Although a preferred option, autologous tissues (tissues taken from other parts of the patient's body) present constraints such as donor site morbidity, muscle weakening, and a limited number of available sites.[7] Similarly, mechanical and prosthetic grafts have a limited life span and often result in inflammation, acute graft thrombogenicity, calcification, and formation of aneurysms.[8, 9] As a result, patients must take anticoagulants for the rest of their life, may require multiple surgeries, and some grafts reportedly fail in pediatric patients, for example, prosthetic heart valves.[10, 11] Therefore, the above options are not the preferred treatment for congenital defects as they lack the ability to grow with pediatric patients.[12]

Tissue engineering works towards solving some of these challenges by mimicking the physiological composition and function of the native tissues.[12-14] An example of a tissue-engineered graft could be one that contains autologous cells expanded from a small piece of donor tissue.[15] The graft can then be cultured under proper

chemical, mechanical, and electrical conditions *in vitro* to develop an engineered tissue with functional and morphological properties similar to those of native tissue.[16, 17]

Most tissues in our bodies encounter a variety of complex mechanical forces. For example, heart valves encounter shear stress, cyclic stretch, and pressure.[18] Researchers often must separate these mechanical forces to better understand each component's contribution on cellular behavior and implement these forces for various tissue engineering applications. Among the various physiological forces, cyclic stretch plays an essential role in the development, maintenance, and function of a variety of tissues.[19] For example, arteries undergo cyclic stretch caused by luminal and abluminal flow.[9] Stretch and other hemodynamic forces in the cardiac cycle have been shown to maintain the heart valves.[20] Bone functionally adapts to physical forces such as stretching, hydrostatic pressure, and bending.[21] Likewise, cyclic stretch induced by filling and emptying is essential to the development of the urinary bladder.[22] Like tissues, cells in culture respond to cyclic stretch in various ways. Cells isolated from connective tissues mostly respond to stretch by aligning themselves in the direction of the applied stress.[23, 24] Additionally, cyclic stretch mediates a variety of cell function: growth factor secretion and calcium handling in cardiomyocytes, calcium wave propagation, and adenosine triphosphate (ATP) release in osteoblast-like cells, to name a few.[25, 26] Cells within aortic valve tissues under stretch expressed increased amounts of α-

smooth muscle actin (αSMA), and their secretion of extracellular matrix proteins was also improved.[27-29] For 3D engineered tissues, cyclic stretch promotes cell proliferation and differentiation, and increases the ultimate tensile strength (UTS) and tensile modulus, which often correlate to increased collagen deposition and maturation.[21, 30, 31]

The goal of engineered tissues is to mimic the functionality of the native tissues and not necessarily their physiology or composition (similar to prosthetic devices). As a result, engineered tissues can be subjected to non-physiologic conditions to achieve some desired properties in the tissues. Various custom bioreactors have been designed for developing functional engineered tissues in a laboratory setting.[32-34] These bioreactor designs have been frequently used for both engineered tissues and mechanobiology studies on tissue strips, for example, for heart valves.[27, 29, 35] In this review, we focused on different designs of stretch bioreactors for tissue engineering, the scaffolds used in these systems, and some of the existing challenges and future directions.

Design of stretch bioreactors

Most bioreactors contain four components: 1) an actuating and motion-transforming system to provide designed stimuli such as stretch and/or electric pulse, shear stress, etc.; 2) a monitoring and control system to capture the loads

and deformations data with sufficient precision and to precisely control the loading profiles; 3) a sample culture chamber to maintain sterility and provide cell/tissue culture environment; and 4) a nutrition exchanging system to circulate new media and remove waste.[36, 37]

Actuating and motion transforming system

The actuating and motion transforming system is the key component for mimicking the native mechanical stretch environment. A variety of actuating units, clasps, and scaffolds have been implemented to achieve the desired stress and strain fields for various tissues of interest. The three most commonly used stretching schemes are motor driven clamps, pressurized-fluid or gas-deformed flexible structures, and shear-stress deformed specimens. Motor driven clamps provide a relatively simple and cheap scheme for applying uniaxial or biaxial stretch with ease of control[6, 26, 35, 38-41] as illustrated in Fig. 7 (A-B). (All tables and figures are located in the appendix.) Uniaxial stretch can be applied on engineered tissues in combination with other stimuli to mimic the native conditions. For example, rotation at one end of the scaffold can be incorporated for engineered tendons and ligaments[42, 43] and electric pulses generated by electrodes are commonly applied to engineered myocardium.[25, 44, 45] For tissue-engineered heart valves, the effects of uniaxial stretch, flexion and shear stress have been studied simultaneously.[20, 29, 46] To precisely control the stretch along two directions, at least two motors must be utilized and controlled independently.[47, 48] For equibiaxial or fixed-ratio-biaxial stretch, both simpler and more frequently studied, the edges of a circular or

elliptically shaped specimen are moved against corresponding plungers.[49, 50] The specimens are stretched uniformly along their outer perimeters, creating an internal strain field that is mostly homogeneous but biaxial. The plungers can be fixed and the edges of specimens can be aspirated to move downward using vacuum pressure; alternatively, the specimens can be fixed and the plungers driven upward by motors, as illustrated in Fig. 7 (C). The movements and forces generated by motors can be precisely monitored and controlled. Digital mini servo rotary stepper motors can rotate 0.09◦/step, while linear motors can reach a microstep size of <0.1μm linear displacement.[47] However, parts connected to motors often must be inserted into the culture chamber to drive the scaffold, which increases the possibility of contamination and generates a lot of heat during operation. To reduce the risk of contamination, a flexible thin latex membrane can be used to separate the walls and inside parts of culture chambers from the rest of the bioreactor components. Although the stepper motors are usually very cheap, the prices of linear motors can be several times higher. In addition, the motion-transforming units can be complex and relatively bulky when motors output rotational motion.

Transforming units are used to translate the rotation of the motor shafts into reciprocating linear motion, as shown in Fig 8. Timing-belt pulleys and engaged gears are structurally very simple, and their linear speeds are determined by the sizes of pulleys or gears.[38, 44] A cam-shaft is robust and can generate great force

at high speeds; however, the speed curves depend on the shaft geometry and are fixed during the operation of a bioreactor.[50-52] A cam can be shaped to be axisymmetric such as a 4-sinusoid waveform superimposed around the circumference of a circle.[53] Thus, it can stretch the scaffold multiple times with each cam rotation. In addition to the classic schemes above, automated linear motion tables and power screw linear actuators are now commercially available.[3, 54-56] Both are based on a rotating lead screw driven by the motor and an attached nut restricted to move along the lead screw linearly. Therefore, they are ready to use and can be precisely controlled by changing the angular speed of a motor via software such as Labview.[3]

Pressurized fluid or gas can be used to apply uniform stretch on 3D thin wall scaffolds, such as scaffolds of engineered hearts,[57, 58] lungs,[2, 59] bladders,[22] or vascular tissues.[30, 60, 61] This usually involves a flexible mandrel or balloon inflated or deflated by a pump. These have frequently been used for engineered vascular tissues, for example.[10] For engineered vascular tissues, the mandrel can be capped at one end and attached to a fixed inlet of pressurized fluid or gas at the other end, as shown in Fig. 7 (D).[9, 62, 63] The expansion of the lumen induces stretch along the radial direction, while stretch along the longitudinal direction can be realized by moving the capped end along the axis of the lumen.[64] If the pressure is strong enough, a pressurized fluid or gas system can even drive multiple samples simultaneously. Unlike motors, which usually work inside incubators and

which can generate substantial amounts of heat, the pumps are kept outside, which eliminates the need for a cooling system and saves space inside incubators. A challenge for systems utilizing pumps is that the stiffness of engineered tissues continually changes during culture due to tissue remodeling and scaffold degradation. Although the volume-strokes and the frequencies of pumps are controllable, since strain is determined by both the forces applied and the stiffness of the scaffold, the pressure will need to be continuously adjusted to maintain the strain amplitude applied to the scaffold.[31, 57]

For cardiovascular tissues such as blood vessels and heart valves, flow induced shear stress is an essential component of the native mechanical environment. Shear stress is a frictional force between a fluid and the surface it flows through. Similar to cyclic stretch, shear stress modulates cellular behavior including endothelial cell alignment, activation of intracellular pathways by affecting integrin, G-protein coupled receptor, tyrosine-kinase receptors and ion channels.[65-67] Therefore, shear-stress-induced stretch devices have frequently been used for developing functional engineered cardiovascular tissues, which have been extensively discussed in previous reviews.[8] Since this review focuses on stretch devices used in tissue engineering applications, flow or shear-stress deformed systems are not discussed. Table 1 summarizes the advantages and limitations of the featured bioreactors we discussed above.

Monitoring and control system

In the past 15 years, monitoring and control systems for stretch bioreactors has remarkably improved. In early stages, the stretch bioreactors contained simple tools to measure changes in force or displacement, since those studies focused on qualitative conclusions. Recent sophisticated bioreactors can obtain detailed quantitative results on a miniature scale, which includes changes in tissue mechanical properties or in the microstructure of the extracellular matrix (ECM). This level of technology, however, requires instruments to gather sufficiently accurate data of the stress and strain field, or automatically obtain microscopic imaging with high efficiency during experiments. Techniques used to monitor the stretch applied on the engineered tissues fall into two main categories: 1) measuring deformations including the displacement, strain fields, and shape/microstructure change of samples and 2) measuring loads including forces, gas or liquid pressure, and stress fields. These measurement techniques are frequently updated to improve the design of monitoring and control systems.

To measure deformations, manual tools such as dial gauges or calipers can be used; these have a resolution of 0.01mm.[51] Strain gauges[68] and inductive displacement transducers (IDT)[45, 50] measure displacements as a change in electrical resistance or induced current. Although easily read, these devices must be mechanically coupled to the moving parts whose position is being measured, which complicates the bioreactor design and increases the risk of contamination.

Alternatively, laser-based micrometers (LBM) can noninvasively monitor by comparing the phase of a transmitted signal of a laser light to the received signal.[41] Thus, the position of a sample can be precisely calculated based on the speed of light. In addition, strain fields are typically monitored by tracking multiple fiducial markers.[48] Simply patterned markers (SPM) can be placed at equal distances on the sample and captured while under stretch using a high-speed camera.[27, 31, 69] However, this method can generate only general strain fields with relatively low resolution. A digital image correlation technique (DIC) can acquire strain fields with high precision by applying marker fields in a random pattern and comparing deformed marker fields to the original based on changes in pixel intensity or gray scale value.[49, 56] Commonly used imaging techniques for monitoring engineered tissues include endoscopic surveillance, magnetic resonance imaging (MRI), or real-time laser scanning (RTLS).[57, 70] In addition, a multimodal nonlinear optical microscopy-optical coherence microscopy (NLOM-OCM) system can be used to noninvasively delineate relative spatial distributions of collagen, fibrin, and cells.[48]

For measuring loads, force transducers are typically based on strain gauges bonded onto a beam or a structural member with a given stiffness.[68, 71] The force transducers used in bioreactors can range from 500 mN to 500 N with an accuracy of 0.03%. The transducers must be placed on opposite sides of the actuating rod to avoid interference during movement.[43, 48] The pressure of flow, another important load type, is usually directly monitored by inline pressure transducers.[9,

[58] In addition, the pressure and velocity of fluids can be obtained using computational fluid dynamic (CFD) simulations and then experimentally validated by particle image velocimetry (PIV). For example, the fluid of interest can be seeded with tracer fluorescent polymer microspheres. A 532-nm laser pulse can then be expanded in a 2mm thick sheet using a spherical and a cylindrical lens and then projected into the fluid. Movement of the microspheres can be captured with a CCD camera for two sets of sequential images within microseconds to map the 3D flow field.[46] Table 2 summarizes the advantages and limitations of the monitoring and control techniques commonly used in stretch bioreactors in literature.

Culture chambers

A culture chamber can provide the required physiological conditions as well as maintain sterility during culture. Engineered tissues often must be cultured *in vitro* for up to 8 weeks[72] to achieve near physiological ECM composition and material properties. Culture duration in stretch bioreactors, however, is often limited by the ability to maintain sterility and the ability of engineered tissue to withstand stretch. The materials used in culture chambers must be biocompatible, corrosion-resistant, easy to clean, and suitable for sterilization.[23] Optical transparency is preferred for macroscopic observation and real-time imaging of processes within the chamber.[70] Because they are completely transparent, acrylic (PMMA),[61, 70, 73] polycarbonate (PC),[46, 74] and glass[72] are most commonly used for chambers. Polydimethylsiloxane (PDMS), a silicone rubber, can be fabricated into optically

clear, flexible structures with an external hydrophobic surface.[75, 76] If real-time microscopy is required, the bioreactor system must fit on top of a microscopic stage and allow for objectives to be positioned within their working distances.[56] For example, nonlinear optical microscopic imaging of developing collagen fibers can be achieved using an imaging window constructed from a glass tube fitted with a piece of optical glass at the bottom. The glass imaging tube is positioned inside a silicone bushing in the chamber, and the imaging window can slide up and down in sterile fashion in close proximity to the engineered vessel to acquire images.[72] In addition, easy sterilization is a requirement for culture chambers, and materials such as polyetherimide (PEI), polysulfone (PSF),[27, 77] polytetrafluoroethylene (PTFE) and polyether ether ketone (PEEK) polymer[25, 54, 55] are commonly used for their stability during autoclaving. PEI can also provide outstanding magnetic susceptibility matching to water if the bioreactor is to be imaged using magnetic resonance imaging (MRI). For load-bearing parts inside chambers, corrosion-resistant stainless steel, titanium, aluminum, and nylon are widely used.[5, 44, 53]

Recently, 3D printing techniques have been thriving since they are economical and can be easily customized.[78] A few culture chambers have been fabricated through stereolithography using acrylic, and the application of 3D printing is very promising for prototyping thin wall structures. Table 3 summarizes commonly used thermoplastics for culture chamber fabrication in tissue engineering applications.

Nutrition exchanging system

Nutrition exchanging systems are used to maintain proper pH, humidity, and concentrations of O_2 and CO_2, as well as to supply metabolites and remove wastes produced by the engineered tissues. Although most bioreactors are designed to be compact enough to fit into an incubator, some bioreactors are larger and have an independent system for maintaining a physiological environment for the engineered tissues.[68] For optimal O_2 and nutrients supplies, the bioreactors often have inlet and outlet ports to provide constant flow of the cell culture medium, which allows metabolites to be transported into deeper cell layers for proper cell survival, growth, and function.[72] Although no definite guideline on culture medium replenishment for bioreactors exists in the literature, the need of medium replacement depends largely on the pH and the potency of additives, such as growth factors, in the culture medium. However, the common practice is to change the medium once every 2 to 3 days.[38, 63, 79]

Stretch regimen

Engineered tissues are commonly cultured under stretch regimens that mimic the physiological mechanical stretch of the tissue of interest. For example, to condition engineered bladders, the pattern of stretch was set based on the bladder activity within a period of 24 h: initially, four sets of filling-emptying in 16 h and then 8 h of rest. In each fill-empty cycle, stretch began from 0 to 2.5% at the beginning of 3 h, followed by 1 h with a larger elongation ranges from 5% to 25%. In the resting cycle, the engineered tissue was cultured under no stretch.[22] For neurons, axons

were grown under stretch by taking a 1μm step every minute over 1000 iterations resulting in 1 mm elongation growth each day.[54]

It is well known that cells adapt to constant environmental stimuli; that is, cellular response to constant mechanical stimulation often reaches a plateau.[54] Therefore, researchers have applied varying stretch regimens, such as a regimen of incremental stretch, to enhance the activity of cells and to strengthen the tissue. Engineered cardiovascular tissues were subjected to cyclic radial stretch, where the strain amplitude incremented from 5% to 15% over the 3 weeks of culture. The strength and stiffness achieved under this stretch regimen were considerably greater (98% for strength and 61% for stiffness) than tissues cultured under constant 15% stretch. Furthermore, the collagen concentration was 34% higher with incremental stretch in comparison with constant stretch.[30] However, there is a dearth of literature that explores variable stretch regimens for engineered tissues; therefore, optimizing stretch regimens may be a promising area for developing functional engineered tissues.

Tissue-engineered scaffolds for stretch bioreactors

Scaffolds influence the mechanical-induced microenvironments (strain, fluid flow, and pressure gradients) acting on cells.[51] Likewise, cells continuously repair and

remodel their tissue microenvironment in response to these mechanical cues. This includes secretion and/or degradation of extracellular matrix proteins, release of soluble growth factors, and reorganization of cell-cell/cell-matrix adhesive interactions, which guides the formation of ECM and tissues.[49] For example, Vickers et al. found that scaffolds with increased stiffness prevented cell-mediated contraction, which resulted in reduced matrix synthesis.[51] Niklason et al. cultured smooth muscle cells (SMC) on a nonwoven scaffold made of polyglycolic acid (PGA) and found that adherent SMC aligned along the long axis of the PGA fibers under static culture condition. Similar alignment along the struts of a micro-molded scaffold and electrospun fibers was reported for porcine valvular interstitial cells (VICs) and myoblasts respectively.[38, 73] In the early stages of stretch before the PGA fibers degraded, collagen fibers aligned along fibers, which suggested that collagen-producing cells secrete collagen along their long axes.[72] Generally, engineered tissues cultured under stretch present elevated cell activity as well as alignment of cells and collagen fibers along the principle stretch direction, regardless of the cell type and the duration of culture. In addition to cell type used, the performance of engineered tissues depends heavily on the scaffold, the profile and frequency of stretch, and the culture duration. Since the subsequent two factors have been discussed in detail in other reviews,[19] this manuscript focuses on the influence of scaffolds to the properties of the engineered tissues. Native tissues exhibit complex, mechanically anisotropic properties and structures optimized for their functions, and there has been a surge of interest in mimicking

the anisotropy of native tissues in recent years.[80] Therefore, different factors that can induce anisotropy in engineered tissues such as anisotropic scaffolds and biaxial stretch are also discussed.

Decellularized tissue scaffolds

Decellularized tissue scaffolds are widely used for many engineered tissues such as tendon, whole hearts, and aortic heart valves.[12, 57, 81, 82] Since these scaffolds can preserve the basic anatomy as well as critical ECM characteristics of the native tissues, they are especially suitable for engineered tissues with complex structures. For example, decellularized rabbit hindpaw based engineered tendons were conditioned under cyclic stretch with a force of 1.25N for 5 days. Being exposed to stretch significantly increased the UTS and stiffness of the engineered tendons compared to unloaded controls.[83] However, it is very difficult to completely remove the cellular remnants, which can induce disease transmission, immunoreactions, calcification, and blood coagulation.[84] To reduce these risks, the decellularized tissues have been modified by various fixatives, such as procyanidins, quercetin, pentagalloyl glucose, glutaraldehyde and methacrylated alginate. Procyanidins and quercetin introduced permanent crosslinks and prevented biodegradation of the matrix.[85, 86] Degradable glutaraldehyde and pentagalloyl glucose fixed tissues showed similar mass loss of collagen to non-fixed tissues, while pentagalloyl glucose could better retain the biaxial mechanical and biological properties in tissues.[82] Crosslinked methacrylated alginate can form an effective non-toxic, flexible coating to allow large deformation and slower

degradation, thus it has been successfully used in decellularized lung segments.[87] Although decellularized tissues have greater advantage in mimicking the anisotropy of native tissues, efforts are still in place to enhance their biocompatibility and tunability of biodegradation and mechanical strength.

Biomaterial scaffolds

Hydrogels such as collagen, chitosan, and fibrin are promising scaffold materials for engineered tissues, owing to their high biochemical and mechanical tunability, customizable degradability, and cell permeability.[53, 72] Collagen is the most commonly used hydrogel since it is the primary insoluble structural protein in the ECM.[1] For example, engineered cardiovascular tissues composed of smooth muscle cells and collagen hydrogel scaffold were conditioned under 5% stretch. After the first 2 weeks of stretch, the UTS and tensile modulus did not increase significantly. However, after 5 weeks, samples exhibited approximately 1.6 fold increases in both UTS and modulus.[62] Fibrin is also favorable since its degradation can be controlled and the cell-secreted collagen content can be measured and used as an indicator of new ECM.[30, 31] For example, human-dermal-fibroblast-seeded fibrin gels as engineered heart valves were cultured under incremental stretch of 5% to 15% over 3 weeks at a frequency of 0.5 Hz. After conditioning, the leaflets manifested anisotropic stiffness with circumferential collagen fiber alignment comparable to native pulmonary leaflets. However, the hydrogel scaffolds often lack in strength and alignment of native collagen fibers; therefore,

they are generally cultured under static tension for 8 to 16 days, allowing for secretion of ECM by the cells to enhance their strength before being stretched.[9, 62]

In addition to hydrogels, biomaterial scaffolds can also be fabricated using a lyophilization process to achieve better mechanical properties.[88, 89] Because of their controllable porosity and degradation, mechanical stability, and ability to swell and fill a void space,[17] lyophilized scaffolds are ideal for engineered tissues that undergo large loads such as engineered bones, cartilage, and heart valves. For example, a chitosan-collagen mixture was lyophilized to form a porous scaffold to create tissue-engineered heart. The scaffold were seeded with neonatal cardiomyocytes and conditioned under equibiaxial stretch for 6 days at a frequency of 1 Hz. The scaffolds exhibited excellent elastic properties and biocompatibility for supporting the cardiomyocytes. Mechanical stimulation further enhanced cell elongation, alignment, and expression of cardiac markers at regions of high local stresses.[51]

Biodegradable polymer scaffolds

Biodegradable polymer fibers such as poly-4-hydroxy-butyrate (P4HB), chitosan-based hyaluronan (HA) hybrid polymer, PGA, and poly(lacticacid) (PLA) have been shown to provide excellent support for cell adhesion and type I collagen production in engineered tissues.[29, 68, 77] They are stronger than hydrogels, and thus can be used to form scaffolds with a strength and stiffness similar to native tissues.[46, 77] For example, engineered human cardiovascular patches were fabricated from

pediatric-aortic-cell-seeded P4HB scaffolds and conditioned under pulsatile stretch with a systolic pressure of 8 mm Hg for 14 days. After conditioning, the scaffolds were partially absorbed and replaced with cell-secreted ECM and exhibited greater strength than static controls.[61]

Techniques to generate anisotropic engineered tissues

Current efforts towards generating anisotropy in engineered tissues can be categorized into two types: 1) fabricating scaffolds with anisotropic properties and 2) applying directional mechanical forces on engineered tissues. Three methods including micro-molding, electrospinning, and 3D printing are primarily used to generate anisotropic scaffolds. Micro-molding can be molded on a variety of materials, such as polydimethylsiloxane(PDMS), poly(glycerolsebacate), and chitosan-collagen.[26, 90] In general, the anisotropic patterns created by micro-molding are relatively simple; however, they might not be suitable for tissues with complex structures. For example, heart valve patches composed of VICs seeded micro-molded poly(glycerol sebacate) scaffolds were cultured under 10% uniaxial stretch at a frequency of 0.36 Hz for 2 weeks. Compared to static controls, these engineered patches showed significant increases in DNA and collagen content, and their stiffness was well maintained while a 40% decrease in stiffness was apparent for static culture.[38]

Electrospinning is the most commonly used technique to prepare tissue-engineered scaffolds due to its versatility, cost-effectiveness, ease of handling, and

applicability to most polymers including polyesterurethane, polymer-chloroform and poly (esterurethane) ureas (PEUU).[74, 91] For example, engineered skeletal muscle constructs were prepared from myoblast- seeded *DegraPol*® electrospinning microfibrous membranes. These constructs were conditioned under 3.4% static stretch following 6.7% cyclic stretch for 13 days at a frequency of 0.5. At day 10, the applied stretching pattern led to an eight-fold increase in myosin accumulation in cyclically stretched constructs with respect to the static controls.[73] However, reducing the fabricating time and tuning orientations of fibers for complex engineered tissues remains a challenge.

3D bioprinting is capable of precisely deploying different cells and materials simultaneously based on a digital model;[92-95] therefore, it has the potential to fabricate complex customized engineered tissues with anisotropy.[96] Stereolithography, ink-jet, or extrusion-based 3D bioprinting are actively studied for 3D printing living cells and scaffolds.[97-103] Stereolithography can reach a resolution up to 1.3 μm while resolutions of ink-jet and extrusion-based 3D bioprinting are only a few hundred μm.[104-107] However, the latter techniques are relatively inexpensive and preferable for fabrication of scaffolds using multiple materials and cells.[105]

Although pulsatile flow can provide critical physiological forces for conditioning functional engineered cardiovascular tissues, directional mechanical forces for

generating tissue anisotrophy has been implemented primarily through biaxial stretch due to the difficulty to precisely control the complex flow field. For example, VICs were encapsulated in ellipsoidal collagen hydrogels, which could be stretched uniformly from the edges. The strains in the X and Y directions (Exx/Eyy) were set as 25%/25%, 20%/40% and 10%/40% respectively. After stretching the engineered gels for 96 h at 1 Hz, the cellular proliferation and apoptosis were both significantly enhanced. While the maximum area strain was kept at 50%, increasing anisotropy of biaxial strain resulted in increased cellular orientation and collagen fiber alignment along the principal directions of strain, and cell orientation was found to precede fiber reorganization.[49] In addition, Bai et al. found that in biaxially stretched fibroblast-seeded fibrin gels (1.0:1.1 stretch ratio), mechanical anisotropy was observed only after decellularization, which suggested that the embedded cells had a homogenizing effect on tissue mechanical properties.[48]

While the applications of anisotropic scaffolds and stretches have shown great potential in generating native-like ECM and cell alignment, most of the research involving stretch still aims to develop functional tissues rather than organs. This is because development of functional engineered organs usually involves complicated angiogenesis as well as formation of endothelial layers, which still require further study

Conclusions and future directions

Various sophisticated designs of stretch bioreactors and scaffolds have contributed greatly to the production of functional engineered tissues and our understanding of tissue formation. For example, PGA/PLA based engineered tendons were stretched with an elongation of 10% *in vitro* before transplantation into rabbits' Achilles tendon sites. Adipose-derived stem-cell-seeded constructs gradually formed neo-tendon and became more mature after 45 weeks with histological similarity to native tendon. Additionally, both collagen fibril diameters and tensile strength increased continuously with significant difference among the different time points.[79] While no controlled clinical trial was found for engineered tissues conditioned by stretch-only bioreactors in the literature, based on the observations from clinical trials without *in vitro* conditioning, inflammation, calcification, and deformation of transplantation site are major barriers to success. In terms of stretch bioreactors, researchers still face challenges including conducting quantitative analysis in real-time to precisely study the mechanical properties and to monitor the formation of tissues, and optimizing stretch regimens, structures, and materials of scaffolds for different kinds of tissue formation. In pursuit of these goals, activity in the following areas should continue:

1) Improvements in biaxial stretch bioreactors: For tissues such as heart valves, blood vessels, and myocardium patches, there is an urgent demand for bioreactors designed to allow precise and independent control along both directions. Two primary schemes have been used to maximize the uniformity

of the applied strain fields. The first involves fixing four edges of a cruciform-shaped scaffold to the actuating arms, as shown in Fig. 7 (B). In this case, the central part of the engineered tissue is subject to biaxial stretch, while the remainder is under uniaxial stretch.[48] The second utilizes rectangular scaffolds, and instead of stretching the entirety of the edges, force is applied at multiple points along each edge using thin wire clips or sutures.[47] However, improvements still could be made in clamping system to increase the effective stretch area and simplify the mounting process before stretch. In addition, a 0% stretch status should be defined to ensure the consistency of the cyclic stretch and facilitate comparison of results from different studies.

2) Development of real-time monitoring systems: To study anisotropic mechanical properties, it is necessary to obtain both real-time strain and stress fields on the tissues. With digital image correlation and a high-speed camera, it is easy to track the deformation and distribution of strain fields with excellent accuracy. However, to calculate stress fields at a specific time point, the precise shapes of each cross section of the tissue are indispensable. Unfortunately, it is difficult to track thickness, since most of the tissues are extremely thin. Therefore, addressing this problem will contribute greatly towards understanding the anisotropy of tissues.
3) Design of hybrid scaffolds: Combining multiple technologies can produce scaffolds to better mimic the anisotropy of native tissues. For example, tri-layered scaffolds were fabricated by assembling micro molded poly(glycerol

sebacate) (PGS) and two layers of fibrous PGS/poly(caprolactone) (PCL) electrospun sheets to develop elastic scaffolds with tunable anisotropic mechanical properties similar to the mechanical characteristics of native heart valves. These scaffolds possessed advantages, namely, reduced production time (micro molding technique) and enhanced permeability of cells (electrospinning).[91]

4) Optimization of materials and stretch regimen for specific engineered tissues: New materials and techniques, such as 3D bioprinting, are now regularly used for bioreactor designs. Hydrogels are the most commonly used material in 3D bioprinting since they are easy to shape and can be cross-linked by UV during or after printing.[108, 109] Some thermoplastics with relatively low melting points are also suitable for 3D bioprinting, for example, P4HB, which has a melting point of about 60°C and a glass transition temperature of 50°C.[61]

In summary, considering the questions that remain unanswered in the field of tissue engineering, we have barely scratched the surface. Both bioreactors and scaffold materials will continue to become optimized and will evolve with time and further research.

References

1. Wang T, Gardiner BS, Lin Z, Rubenson J, Kirk TB, Wang A, Xu J, Smith DW, Lloyd DG, Zheng MH. Bioreactor design for tendon/ligament engineering. Tissue Eng Part B Rev. 2013;19:133-146.
2. Price AP, England KA, Matson AM, Blazar BR, Panoskaltsis-Mortari A. Development of a decellularized lung bioreactor system for bioengineering the lung: the matrix reloaded. Tissue Eng Part A. 2010;16:2581-2591.
3. Ritchie AC, Wijaya S, Ong WF, Zhong SP, Chian KS. Dependence of alignment direction on magnitude of strain in esophageal smooth muscle cells. Biotechnol Bioeng. 2009;102:1703-1711.
4. Cui X, Boland T, D'Lima DD, Lotz MK. Thermal inkjet printing in tissue engineering and regenerative medicine. Recent patents on drug delivery & formulation. 2012;6:149.
5. McKeen LW. Plastics Used in Medical Devices. 2014:21-53.
6. Noth U, Schupp K, Heymer A, Kall S, Jakob F, Schutze N, Baumann B, Barthel T, Eulert J, Hendrich C. Anterior cruciate ligament constructs fabricated from human mesenchymal stem cells in a collagen type I hydrogel. Cytotherapy. 2005;7:447-455.
7. Gaspar DA, Gomide V, Monteiro FJ. The role of perfusion bioreactors in bone tissue engineering. Biomatter. 2012;2:167-175.
8. Berry JL, Steen JA, Koudy Williams J, Jordan JE, Atala A, Yoo JJ. Bioreactors for development of tissue engineered heart valves. Ann Biomed Eng. 2010;38:3272-3279.
9. Syedain ZH, Meier LA, Bjork JW, Lee A, Tranquillo RT. Implantable arterial grafts from human fibroblasts and fibrin using a multi-graft pulsed flow-stretch bioreactor with noninvasive strength monitoring. Biomaterials. 2011;32:714-722.
10. Perri G, Polito A Fau - Esposito C, Esposito C Fau - Albanese SB, Albanese Sb Fau - Francalanci P, Francalanci P Fau - Pongiglione G, Pongiglione G Fau - Carotti A, Carotti A. Early and late failure of tissue-engineered pulmonary valve

conduits used for right ventricular outflow tract reconstruction in patients with congenital heart disease.

11. Ruffer A, Purbojo A Fau - Cicha I, Cicha I Fau - Glockler M, Glockler M Fau - Potapov S, Potapov S Fau - Dittrich S, Dittrich S Fau - Cesnjevar RA, Cesnjevar RA. Early failure of xenogenous de-cellularised pulmonary valve conduits--a word of caution!

12. Rippel RA, Ghanbari H, Seifalian AM. Tissue-engineered heart valve: future of cardiac surgery. World J Surg. 2012;36:1581-1591.

13. Schenke-Layland K, Walles H. Strategies in tissue engineering and regenerative medicine. Biotechnol J. 2013;8:278-279.

14. Vunjak‐Novakovic G, Meinel L, Altman G, Kaplan D. Bioreactor cultivation of osteochondral grafts. Orthodontics & craniofacial research. 2005;8:209-218.

15. Sodian R, Lemke T, Loebe M, Hoerstrup SP, Potapov EV, Hausmann H, Meyer R, Hetzer R. New pulsatile bioreactor for fabrication of tissue‐engineered patches. Journal of biomedical materials research. 2001;58:401-405.

16. Kasper C, Griensven M, Pörtner R. Bioreactor systems for tissue engineering: Springer; 2009.

17. Zhang T, Wan LQ, Xiong Z, Marsano A, Maidhof R, Park M, Yan Y, Vunjak‐Novakovic G. Channelled scaffolds for engineering myocardium with mechanical stimulation. Journal of tissue engineering and regenerative medicine. 2012;6:748-756.

18. Engelmayr GC, Jr., Sales Vl Fau - Mayer JE, Jr., Mayer Je Jr Fau - Sacks MS, Sacks MS. Cyclic flexure and laminar flow synergistically accelerate mesenchymal stem cell-mediated engineered tissue formation: Implications for engineered heart valve tissues.

19. Riehl BD, Park JH, Kwon IK, Lim JY. Mechanical stretching for tissue engineering: two-dimensional and three-dimensional constructs. Tissue Eng Part B Rev. 2012;18:288-300.

20. Thayer P, Balachandran K, Rathan S, Yap CH, Arjunon S, Jo H, Yoganathan AP. The effects of combined cyclic stretch and pressure on the aortic valve interstitial cell phenotype. Ann Biomed Eng. 2011;39:1654-1667.
21. Ignatius A, Blessing H, Liedert A, Schmidt C, Neidlinger-Wilke C, Kaspar D, Friemert B, Claes L. Tissue engineering of bone: effects of mechanical strain on osteoblastic cells in type I collagen matrices. Biomaterials. 2005;26:311-318.
22. Luo Y, Wazir R, Du C, Tian Y, Yue X, Wei TQ, Wang KJ. Magnitude-dependent proliferation and contractility modulation of human bladder smooth muscle cells under physiological stretch. World J Urol. 2015.
23. Barron V, Brougham C, Coghlan K, McLucas E, O'Mahoney D, Stenson-Cox C, McHugh PE. The effect of physiological cyclic stretch on the cell morphology, cell orientation and protein expression of endothelial cells. J Mater Sci Mater Med. 2007;18:1973-1981.
24. Wilke M, Sohn J-H, Byars AW, Holland SK. Bright spots: correlations of gray matter volume with IQ in a normal pediatric population. NeuroImage. 2003;20:202-215.
25. Lu L, Mende M, Yang X, Korber HF, Schnittler HJ, Weinert S, Heubach J, Werner C, Ravens U. Design and validation of a bioreactor for simulating the cardiac niche: a system incorporating cyclic stretch, electrical stimulation, and constant perfusion. Tissue Eng Part A. 2013;19:403-414.
26. Jones BF, Wall ME, Carroll RL, Washburn S, Banes AJ. Ligament cells stretch-adapted on a microgrooved substrate increase intercellular communication in response to a mechanical stimulus. J Biomech. 2005;38:1653-1664.
27. Balachandran K, Konduri S, Sucosky P, Jo H, Yoganathan AP. An ex vivo study of the biological properties of porcine aortic valves in response to circumferential cyclic stretch. Ann Biomed Eng. 2006;34:1655-1665.
28. Merryman WD, Lukoff HD, Long RA, Engelmayr GC, Hopkins RA, Sacks MS. Synergistic effects of cyclic tension and transforming growth factor-β1 on the aortic valve myofibroblast. Cardiovascular Pathology. 2007;16:268-276.

29. Engelmayr GC, Jr., Sales VL, Mayer JE, Jr., Sacks MS. Cyclic flexure and laminar flow synergistically accelerate mesenchymal stem cell-mediated engineered tissue formation: Implications for engineered heart valve tissues. Biomaterials. 2006;27:6083-6095.
30. Syedain ZH, Weinberg JS, Tranquillo RT. Cyclic distension of fibrin-based tissue constructs: evidence of adaptation during growth of engineered connective tissue. Proc Natl Acad Sci U S A. 2008;105:6537-6542.
31. Syedain ZH, Tranquillo RT. Controlled cyclic stretch bioreactor for tissue-engineered heart valves. Biomaterials. 2009;30:4078-4084.
32. Salehi-Nik N, Amoabediny G, Pouran B, Tabesh H, Shokrgozar MA, Haghighipour N, Khatibi N, Anisi F, Mottaghy K, Zandieh-Doulabi B. Engineering parameters in bioreactor's design: a critical aspect in tissue engineering. Biomed Res Int. 2013;2013:762132.
33. Ebrahimkhani MR, Neiman JA, Raredon MS, Hughes DJ, Griffith LG. Bioreactor technologies to support liver function in vitro. Adv Drug Deliv Rev. 2014;69-70:132-157.
34. Yeatts AB, Choquette DT, Fisher JP. Bioreactors to influence stem cell fate: augmentation of mesenchymal stem cell signaling pathways via dynamic culture systems. Biochim Biophys Acta. 2013;1830:2470-2480.
35. Balachandran K, Sucosky P, Jo H, Yoganathan AP. Elevated cyclic stretch alters matrix remodeling in aortic valve cusps: implications for degenerative aortic valve disease. Am J Physiol Heart Circ Physiol. 2009;296:H756-764.
36. Korossis S, Bolland F, Kearney J, Fisher J, Ingham E. Bioreactors in tissue engineering. Topics Tissue Eng. 2005;2:1-23.
37. Partap S, O'Brien F, Plunkett N. Bioreactors in tissue engineering: INTECH Open Access Publisher; 2010.
38. Masoumi N, Howell MC, Johnson KL, Niesslein MJ, Gerber G, Engelmayr GC, Jr. Design and testing of a cyclic stretch and flexure bioreactor for evaluating engineered heart valve tissues based on poly(glycerol sebacate) scaffolds. Proc Inst Mech Eng H. 2014;228:576-586.

39. Balachandran K, Sucosky P, Jo H, Yoganathan AP. Elevated cyclic stretch induces aortic valve calcification in a bone morphogenic protein-dependent manner. Am J Pathol. 2010;177:49-57.
40. Paxton JZ, Hagerty P, Andrick JJ, Baar K. Optimizing an intermittent stretch paradigm using ERK1/2 phosphorylation results in increased collagen synthesis in engineered ligaments. Tissue Eng Part A. 2012;18:277-284.
41. Birla RK, Huang YC, Dennis RG. Development of a novel bioreactor for the mechanical loading of tissue-engineered heart muscle. Tissue Eng. 2007;13:2239-2248.
42. Kahn C, Vaquette C, Rahouadj R, Wang X. A novel bioreactor for ligament tissue engineering. Bio-medical materials and engineering. 2007;18:283-287.
43. Sawaguchi N, Majima T, Funakoshi T, Shimode K, Harada K, Minami A, Nishimura S. Effect of cyclic three-dimensional strain on cell proliferation and collagen synthesis of fibroblast-seeded chitosan-hyaluronan hybrid polymer fiber. J Orthop Sci. 2010;15:569-577.
44. Zhonggang F, Matsumoto T, Nomura Y, Nakamura T. An electro-tensile bioreactor for 3-D culturing of cardiomyocytes. IEEE Engineering in Medicine and Biology Magazine. 2005;24:73-79.
45. Kensah G, Gruh I, Viering J, Schumann H, Dahlmann J, Meyer H, Skvorc D, Bar A, Akhyari P, Heisterkamp A, Haverich A, Martin U. A novel miniaturized multimodal bioreactor for continuous in situ assessment of bioartificial cardiac tissue during stimulation and maturation. Tissue Eng Part C Methods. 2011;17:463-473.
46. Engelmayr GC, Jr., Soletti L, Vigmostad SC, Budilarto SG, Federspiel WJ, Chandran KB, Vorp DA, Sacks MS. A novel flex-stretch-flow bioreactor for the study of engineered heart valve tissue mechanobiology. Ann Biomed Eng. 2008;36:700-712.
47. Metzler SA, Digesu CS, Howard JI, Filip To SD, Warnock JN. Live en face imaging of aortic valve leaflets under mechanical stress. Biomech Model Mechanobiol. 2012;11:355-361.

48. Huang H-S, Huang S, editors. Real-time strain mapping via biaxial stretching in heart valve tissues. Engineering in Medicine and Biology Society (EMBC), 2012 Annual International Conference of the IEEE; 2012: IEEE.
49. Bai Y, Lee PF, Humphrey JD, Yeh AT. Sequential multimodal microscopic imaging and biaxial mechanical testing of living multicomponent tissue constructs. Ann Biomed Eng. 2014;42:1791-1805.
50. Gould RA, Chin K, Santisakultarm TP, Dropkin A, Richards JM, Schaffer CB, Butcher JT. Cyclic strain anisotropy regulates valvular interstitial cell phenotype and tissue remodeling in three-dimensional culture. Acta Biomater. 2012;8:1710-1719.
51. Lau JJ, Wang RM, Black LD, 3rd. Development of an arbitrary waveform membrane stretcher for dynamic cell culture. Ann Biomed Eng. 2014;42:1062-1073.
52. McMahon LA, Reid AJ, Campbell VA, Prendergast PJ. Regulatory effects of mechanical strain on the chondrogenic differentiation of MSCs in a collagen-GAG scaffold: experimental and computational analysis. Ann Biomed Eng. 2008;36:185-194.
53. Gupta V, Werdenberg JA, Lawrence BD, Mendez JS, Stephens EH, Grande-Allen KJ. Reversible secretion of glycosaminoglycans and proteoglycans by cyclically stretched valvular cells in 3D culture. Ann Biomed Eng. 2008;36:1092-1103.
54. Loverde JR, Tolentino RE, Pfister BJ. Axon stretch growth: the mechanotransduction of neuronal growth. J Vis Exp. 2011.
55. Xu Q, Chen F, Wang Y, Li X, He J, editors. Development of a miniaturized bioreactor for neural culture and axon stretch growth. Engineering in Medicine and Biology Society (EMBC), 2014 36th Annual International Conference of the IEEE; 2014: IEEE.
56. Van Dyke WS, Sun X, Richard AB, Nauman EA, Akkus O. Novel mechanical bioreactor for concomitant fluid shear stress and substrate strain. J Biomech. 2012;45:1323-1327.

57. Hulsmann J, Aubin H, Kranz A, Godehardt E, Munakata H, Kamiya H, Barth M, Lichtenberg A, Akhyari P. A novel customizable modular bioreactor system for whole-heart cultivation under controlled 3D biomechanical stimulation. J Artif Organs. 2013;16:294-304.
58. Miklas JW, Nunes SS, Sofla A, Reis LA, Pahnke A, Xiao Y, Laschinger C, Radisic M. Bioreactor for modulation of cardiac microtissue phenotype by combined static stretch and electrical stimulation. Biofabrication. 2014;6:024113.
59. Morgan KY, Black LD, 3rd. Mimicking isovolumic contraction with combined electromechanical stimulation improves the development of engineered cardiac constructs. Tissue Eng Part A. 2014;20:1654-1667.
60. Dassow C, Wiechert L, Martin C, Schumann S, Muller-Newen G, Pack O, Guttmann J, Wall WA, Uhlig S. Biaxial distension of precision-cut lung slices. J Appl Physiol (1985). 2010;108:713-721.
61. Bilodeau K, Couet F, Boccafoschi F, Mantovani D. Design of a perfusion bioreactor specific to the regeneration of vascular tissues under mechanical stresses. Artificial organs. 2005;29:906-912.
62. Yang C, Sodian R, Fu P, Luders C, Lemke T, Du J, Hubler M, Weng Y, Meyer R, Hetzer R. In vitro fabrication of a tissue engineered human cardiovascular patch for future use in cardiovascular surgery. Ann Thorac Surg. 2006;81:57-63.
63. Isenberg BC, Tranquillo RT. Long-Term Cyclic Distention Enhances the Mechanical Properties of Collagen-Based Media-Equivalents. Annals of Biomedical Engineering. 2003;31:937-949.
64. Weidenhamer NK, Tranquillo RT. Influence of cyclic mechanical stretch and tissue constraints on cellular and collagen alignment in fibroblast-derived cell sheets. Tissue Eng Part C Methods. 2013;19:386-395.
65. Marcous S. Developing a Bioreactor for Biaxial Mechanical Testing and Conditioning of Vascular Tissue. 2014.
66. Govoni M, Lotti F, Biagiotti L, Lannocca M, Pasquinelli G, Valente S, Muscari C, Bonafe F, Caldarera CM, Guarnieri C, Cavalcanti S, Giordano E. An

innovative stand-alone bioreactor for the highly reproducible transfer of cyclic mechanical stretch to stem cells cultured in a 3D scaffold. J Tissue Eng Regen Med. 2014;8:787-793.

67. Konig F, Hollweck T, Pfeifer S, Reichart B, Wintermantel E, Hagl C, Akra B. A Pulsatile Bioreactor for Conditioning of Tissue-Engineered Cardiovascular Constructs under Endoscopic Visualization. J Funct Biomater. 2012;3:480-496.

68. Courtney T, Sacks MS, Stankus J, Guan J, Wagner WR. Design and analysis of tissue engineering scaffolds that mimic soft tissue mechanical anisotropy. Biomaterials. 2006;27:3631-3638.

69. Niklason LE, Yeh AT, Calle EA, Bai Y, Valentin A, Humphrey JD. Enabling tools for engineering collagenous tissues integrating bioreactors, intravital imaging, and biomechanical modeling. Proc Natl Acad Sci U S A. 2010;107:3335-3339.

70. Candiani G, Riboldi Sa Fau - Sadr N, Sadr N Fau - Lorenzoni S, Lorenzoni S Fau - Neuenschwander P, Neuenschwander P Fau - Montevecchi FM, Montevecchi Fm Fau - Mantero S, Mantero S. Cyclic mechanical stimulation favors myosin heavy chain accumulation in engineered skeletal muscle constructs.

71. Kluge JA, Leisk GG, Cardwell RD, Fernandes AP, House M, Ward A, Dorfmann AL, Kaplan DL. Bioreactor system using noninvasive imaging and mechanical stretch for biomaterial screening. Ann Biomed Eng. 2011;39:1390-1402.

72. Moraes C, Likhitpanichkul M, Lam CJ, Beca BM, Sun Y, Simmons CA. Microdevice array-based identification of distinct mechanobiological response profiles in layer-specific valve interstitial cells. Integr Biol (Camb). 2013;5:673-680.

73. Tomer NS. Oxidation, Chain Scission and Cross-Linking Studies of Polysiloxanes upon Ageings. Open Journal of Organic Polymer Materials. 2012;02:13-22.

74. Ramaswamy S, Boronyak SM, Le T, Holmes A, Sotiropoulos F, Sacks MS. A novel bioreactor for mechanobiological studies of engineered heart valve tissue

formation under pulmonary arterial physiological flow conditions. J Biomech Eng. 2014;136:121009.

75. Lee JW, Kim JY, Cho D-W. Solid free-form fabrication technology and its application to bone tissue engineering. International journal of stem cells. 2010;3:85.

76. Deng D, Wang W, Wang B, Zhang P, Zhou G, Zhang WJ, Cao Y, Liu W. Repair of Achilles tendon defect with autologous ASCs engineered tendon in a rabbit model. Biomaterials. 2014;35:8801-8809.

77. Hammer PE, Pacak CA, Howe RD, del Nido PJ. Straightening of curved pattern of collagen fibers under load controls aortic valve shape. J Biomech. 2014;47:341-346.

78. Saber S, Zhang AY, Ki SH, Lindsey DP, Smith RL, Riboh J, Pham H, Chang J. Flexor tendon tissue engineering: bioreactor cyclic strain increases construct strength. Tissue Engineering Part A. 2010;16:2085-2090.

79. Sierad LN, Simionescu A, Albers C, Chen J, Maivelett J, Tedder ME, Liao J, Simionescu DT. Design and Testing of a Pulsatile Conditioning System for Dynamic Endothelialization of Polyphenol-Stabilized Tissue Engineered Heart Valves. Cardiovasc Eng Technol. 2010;1:138-153.

80. Saber S, Zhang Ay Fau - Ki SH, Ki Sh Fau - Lindsey DP, Lindsey Dp Fau - Smith RL, Smith Rl Fau - Riboh J, Riboh J Fau - Pham H, Pham H Fau - Chang J, Chang J. Flexor tendon tissue engineering: bioreactor cyclic strain increases construct strength.

81. Bijonowski BM, Miller WM, Wertheim JA. Bioreactor design for perfusion-based, highly-vascularized organ regeneration. Curr Opin Chem Eng. 2013;2:32-40.

82. Wagner D, Fenn S, Bonenfant N, Marks E, Borg Z, Saunders P, Oldinski R, Weiss D. Design and Synthesis of an Artificial Pulmonary Pleura for High Throughput Studies in Acellular Human Lungs. Cel Mol Bioeng. 2014;7:184-195.

83. Feng Z, Tateishi Y, Nomura Y, Kitajima T, Nakamura T. Construction of fibroblast-collagen gels with orientated fibrils induced by static or dynamic stress: toward the fabrication of small tendon grafts. J Artif Organs. 2006;9:220-225.
84. Rodriguez IA, Sell SA, McCool JM, Saxena G, Spence AJ, Bowlin GL. A preliminary evaluation of lyophilized gelatin sponges, enhanced with platelet-rich plasma, hydroxyapatite and chitin whiskers for bone regeneration. Cells. 2013;2:244-265.
85. Bn B. Structural Alterations in Scaffold Architecture in Response to Mechanical Stimuli. Journal of Tissue Science & Engineering. 2012;03.
86. Zhang T, Wan LQ, Xiong Z, Marsano A, Maidhof R, Park M, Yan Y, Vunjak-Novakovic G. Channelled scaffolds for engineering myocardium with mechanical stimulation. J Tissue Eng Regen Med. 2012;6:748-756.
87. Masoumi N, Annabi N, Assmann A, Larson BL, Hjortnaes J, Alemdar N, Kharaziha M, Manning KB, Mayer JE, Jr., Khademhosseini A. Tri-layered elastomeric scaffolds for engineering heart valve leaflets. Biomaterials. 2014;35:7774-7785.
88. Wust S, Muller R, Hofmann S. Controlled Positioning of Cells in Biomaterials-Approaches Towards 3D Tissue Printing. J Funct Biomater. 2011;2:119-154.
89. Chang CC, Boland ED, Williams SK, Hoying JB. Direct-write bioprinting three-dimensional biohybrid systems for future regenerative therapies. J Biomed Mater Res B Appl Biomater. 2011;98:160-170.
90. Williams SK, Touroo JS, Church KH, Hoying JB. Encapsulation of adipose stromal vascular fraction cells in alginate hydrogel spheroids using a direct-write three-dimensional printing system. Biores Open Access. 2013;2:448-454.
91. Mannoor MS, Jiang Z, James T, Kong YL, Malatesta KA, Soboyejo WO, Verma N, Gracias DH, McAlpine MC. 3D printed bionic ears. Nano Lett. 2013;13:2634-2639.
92. Miller JS, Stevens KR, Yang MT, Baker BM, Nguyen DH, Cohen DM, Toro E, Chen AA, Galie PA, Yu X, Chaturvedi R, Bhatia SN, Chen CS. Rapid casting of

patterned vascular networks for perfusable engineered three-dimensional tissues. Nat Mater. 2012;11:768-774.

93. Pati F, Jang J, Ha DH, Won Kim S, Rhie JW, Shim JH, Kim DH, Cho DW. Printing three-dimensional tissue analogues with decellularized extracellular matrix bioink. Nat Commun. 2014;5:3935.

94. Fu Q, Saiz E, Tomsia AP. Direct ink writing of highly porous and strong glass scaffolds for load-bearing bone defects repair and regeneration. Acta Biomater. 2011;7:3547-3554.

95. Villar G, Graham AD, Bayley H. A tissue-like printed material. Science. 2013;340:48-52.

96. Soman P, Fozdar DY, Lee JW, Phadke A, Varghese S, Chen S. A Three-dimensional Polymer Scaffolding Material Exhibiting a Zero Poisson's Ratio. Soft Matter. 2012;8:4946-4951.

97. Mironov V, Visconti RP, Kasyanov V, Forgacs G, Drake CJ, Markwald RR. Organ printing: tissue spheroids as building blocks. Biomaterials. 2009;30:2164-2174.

98. Cui X, Breitenkamp K, Finn MG, Lotz M, D'Lima DD. Direct human cartilage repair using three-dimensional bioprinting technology. Tissue Eng Part A. 2012;18:1304-1312.

99. Soman P, Chung PH, Zhang AP, Chen S. Digital microfabrication of user-defined 3D microstructures in cell-laden hydrogels. Biotechnology and Bioengineering. 2013;110:3038-3047.

100. Poldervaart MT, Wang H, van der Stok J, Weinans H, Leeuwenburgh SC, Oner FC, Dhert WJ, Alblas J. Sustained release of BMP-2 in bioprinted alginate for osteogenicity in mice and rats. PLoS One. 2013;8:e72610.

101. He Y, Xue GH, Fu JZ. Fabrication of low cost soft tissue prostheses with the desktop 3D printer. Sci Rep. 2014;4:6973.

102. Markstedt K, Mantas A, Tournier I, Martínez Ávila H, Hägg D, Gatenholm P. 3D Bioprinting Human Chondrocytes with Nanocellulose–Alginate Bioink for

Cartilage Tissue Engineering Applications. Biomacromolecules. 2015;16:1489-1496.
103. Gurkan UA, El Assal R, Yildiz SE, Sung Y, Trachtenberg AJ, Kuo WP, Demirci U. Engineering anisotropic biomimetic fibrocartilage microenvironment by bioprinting mesenchymal stem cells in nanoliter gel droplets. Mol Pharm. 2014;11:2151-2159.
104. Zhao L, Lee VK, Yoo SS, Dai G, Intes X. The integration of 3-D cell printing and mesoscopic fluorescence molecular tomography of vascular constructs within thick hydrogel scaffolds. Biomaterials. 2012;33:5325-5332.
105. Hockaday LA, Kang KH, Colangelo NW, Cheung PY, Duan B, Malone E, Wu J, Girardi LN, Bonassar LJ, Lipson H, Chu CC, Butcher JT. Rapid 3D printing of anatomically accurate and mechanically heterogeneous aortic valve hydrogel scaffolds. Biofabrication. 2012;4:035005.

Appendix

Table 1. Features of common stretch bioreactors

Source of Stretch	Advantages	Limitations	Actuating system	Type of stretch	Features	Reference
Motor	Precise control Relatively low cost Easily combined with other stimuli Compact	Higher possibility of contamination Extra heat generation within incubators Generally complex motion-transforming units	Motor driven clamps	Uniaxial	Linear actuator	20, 27, 29, 40, 41, 43, 54
					Cam	6, 25, 51
					Linear motor	45
					Coupled gears	38
					Timing-belt pulley	44
			Motor driven clamps	Equibiaxial	Cam	52, 53
			Plunger deformed membrane	Fixed-ratio biaxial	Moving plunger	49, 50
			Motor driven clamps	Individually-controlled biaxial	Two actuators	47, 48
Pump	Easily drive multiple samples Easier to maintain sterile condition	Difficult to precisely monitor and control	Pneumatically deformed mandrel	Uniaxial	Free capped end	58, 62, 63
				Biaxial	Fixed capped end	72
				Biaxial	Controlled capped end	110
			Pneumatically deformed balloon	Biaxial	3D thin wall scaffold	2, 57

Table 2. Commonly used monitoring and control systems in stretch bioreactors

Measurement technique	Measuring variables	Advantages	Limitations
Dial gauges / Calipers	Displacement	Good resolution of 0.01mm	Limited data collection due to manual operation
Strain gauges	Displacement	Low cost, ease of operation error < ±0.1%	Need to be coupled with shafts, Bulky
IDT	Displacement	Robust, high reliability, error < ±0.25%,	Need to be coupled with shafts, Bulky
LBM	Displacement	High resolution of 0.01μm, operates independently	High cost
SPM	Strain field	Ease of operation	Low resolution
DIC	Strain field	High resolution	Relatively complicated setup
Endoscopy	Image of tissue	Real time colorful imaging	Invasive technique
MRI	Image of tissue	Contrast between different tissues, noninvasive	Requires magnetic compatibility of chambers
RTLS	Image of tissue	High accuracy, noninvasive	Limited sampling rate for moving tissues
NLOM-OCM	Fibers in ECM	Real time monitoring of ECM deposition	Special design needed for microscope lenses
Force transducer	Force	Error < ±0.03%	Need to be coupled with shafts
Pressure transducer	Pressure	Simple, installed outside culture chamber	Cannot obtain specific details of fluid field
CFD and PIV	Fluid field	Can map detailed fluid field	Complicated operation

Table 3. Commonly used thermoplastics for chamber fabrication

Material	Appearance	UV sterilization	Gas sterilization	Autoclave	Max temperature (°C)
PMMA	Clear	Yes	Yes	No	50
PC	Clear	No	Yes	Yes	121
PSF	Amber to transparent	No	Yes	Yes	150
PTFE	Opaque	Yes	Yes	Yes	250
PDMS	Clear	No	Yes	Yes	200
PEI	Amber to transparent	Yes	Yes	Yes	216
PEEK	Opaque	No	Yes	Yes	143
Nylon	Translucent	Yes	Yes	No	99

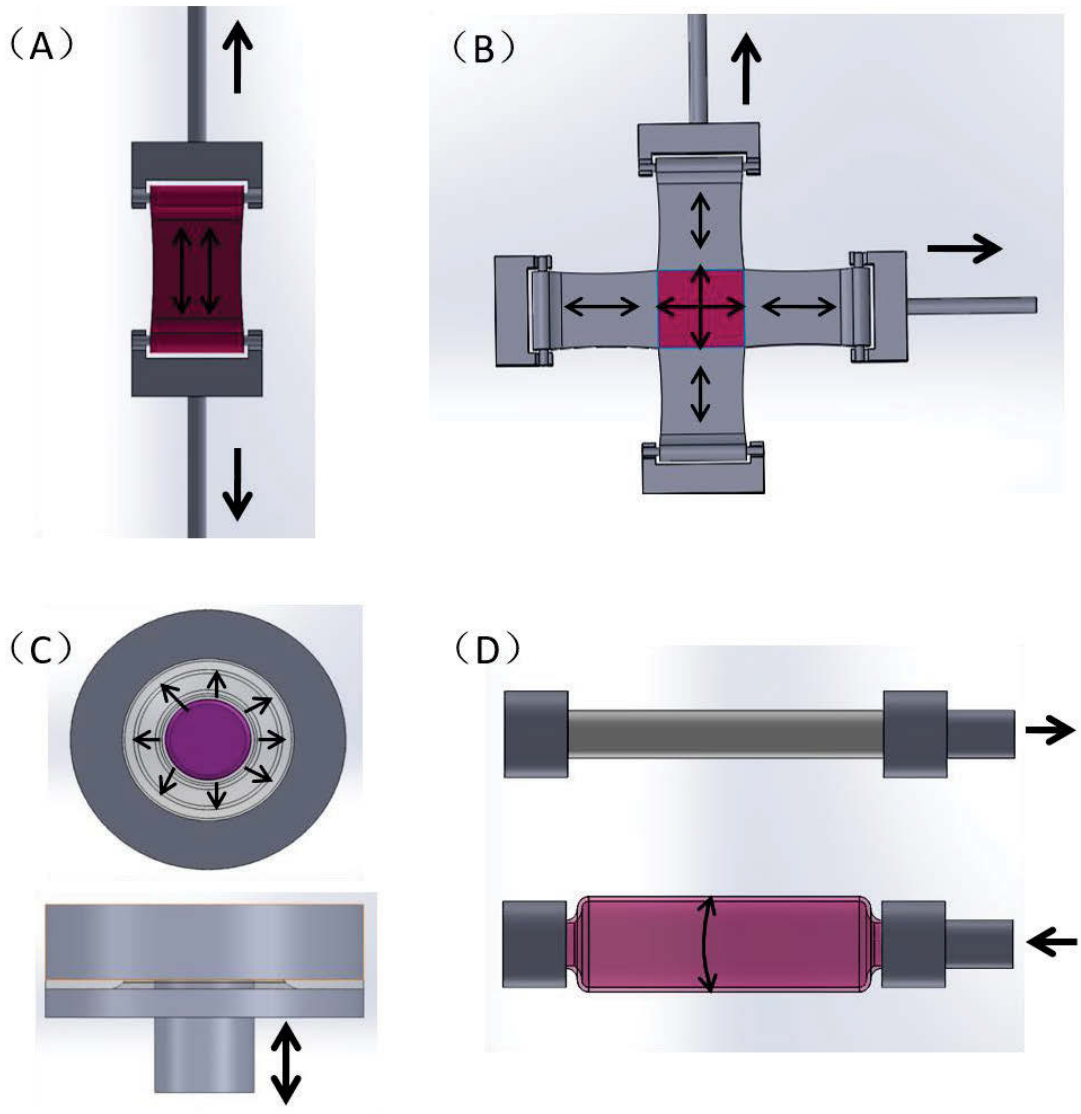


Figure 7. Different actuating units for stretch bioreactors:

(A) Motor driven clamps (Uniaxial); (B) Motor driven clamps (Biaxial); (C) Moving plunger stretching a membrane; (D) Pressurized fluid or gas stretching a tube.

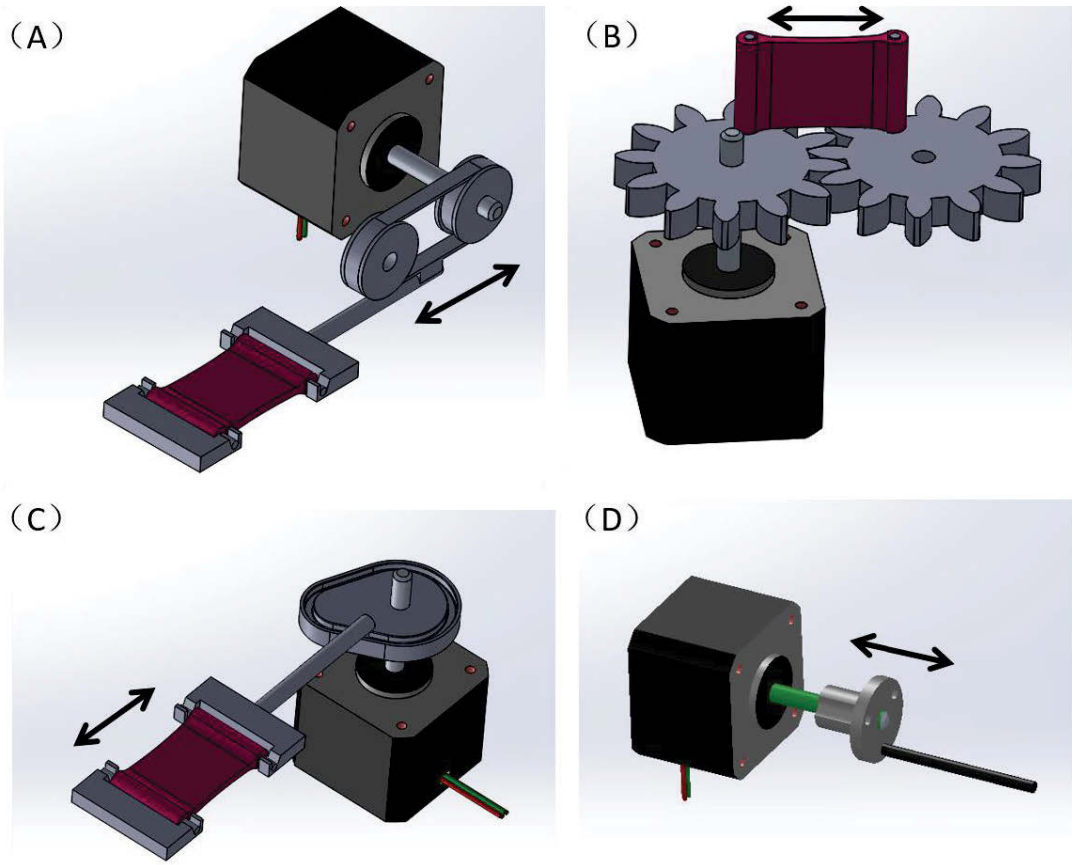


Figure 8. Different Transforming units for linear motions:

(A) Timing-belt pulley; (B) Engaged gears; (C) Cam-shaft units; (D) Power screw linear actuator.

CHAPTER II
A STUDY OF EXTRACELLULAR MATRIX REMODELING IN AORTIC HEART VALVES USING A NOVEL BIAXIAL STRETCH BIOREACTOR

A version of this chapter was originally published by Ying Lei, Shirin Masjedi and Zannatul Ferouds:

Ying Lei, Shirin Masjedi and Zannatul Ferdous. “A Study of Extracellular Matrix Remodeling in Aortic Heart Valves Using a Novel Biaxial Stretch Bioreactor.” *Journal of the Mechanical Behavior of Biomedical Materials.* 75(2017): 351-358.

Ying Lei was responsible for literature review, bioreactor design, fabrication and validation, as well as experimental design, tissue and cell culture, biochemical assays, data collection and analysis, and manuscript drafting. Shirin Masjedi was responsible for histology and biochemical assays. Zannatul Ferdous was responsible for draft submission and revision.

Abstract

In aortic valves, biaxial cyclic stretch is known to modulate cell differentiation, extracellular matrix (ECM) synthesis and organization. We designed a novel bioreactor that can apply independent and precise stretch along radial and circumferential directions in a tissue culture environment. While this bioreactor can be used for either native or engineered tissues, this study determined matrix remodeling and strain distribution of aortic cusps after culturing under biaxial stretch for 14 days. The contents of collagen and glycosaminoglycans were

determined using standard biochemical assays and compared with fresh controls. Strain fields in static cusps were more uniform than those in stretched cusps, which indicated degradation of the ECM fibers. The glycosaminoglycan content was significantly elevated in the static control as compared to fresh or stretched cusps, but no difference was observed in collagen content among the groups. The strain profile of freshly isolated fibrosa vs. ventricularis and left, right, and noncoronary cusps were also determined by Digital Image Correlation technique. Distinct strain patterns were observed under stretch on fibrosa and ventricularis sides and among the three cusps. This work highlights the critical role of the anisotropic ECM structure for proper functions of native aortic valves and the beneficial effects of biaxial stretch for maintenance of the native ECM structure.

Key Terms: Digital Image Correlation, Biaxial stretch bioreactor, Strain patterns, Collagen, Glycosaminoglycan

Introduction

Aortic valves experience unique bidirectional stretch *in vivo*, where the cusps encounter approximately 13–25% strain in the radial direction and 10% strain in the circumferential direction.[45] This physiological strain profile is critical for regulating the cell turnover and alignment in healthy aortic valves.[5] It also guides extracellular matrix (ECM) fibers to be organized in radial and circumferential directions within the cusps, which is necessary for the proper coaptation of

valves.[13] On the other hand, pathological stretch condition causes elevated cell proliferation and apoptosis rate, increased proteolytic enzyme activities, and calcifications in diseased aortic valves.[6, 19, 24] To mimic these stretch conditions in a tissue culture environment, a variety of uniaxial and biaxial stretch bioreactors have been used for tissue engineering and mechanobiology studies of aortic valves.[25] Effects of uniaxial stretch have been extensively studied, alone or in combination with other mechanical stimuli such as flexure, flow-based shear stress or pressure.[10, 11, 28, 32, 34, 39] While biaxial stretch best mimics the stretch environment of aortic valves, the majority of these biaxial devices are designed to apply equibiaxial cyclic stretch.[12, 15] Recently reported bioreactors applied anisotropic strain profile to valvular cell-seeded engineered tissues by modifying either cell orientation patterns[38] or the shape of collagen gels (circular vs. ellipsoidal, major/minor axis ratios 1:1, 2:1, and 4:1) cultured under equibiaxial strain.[13] The control on the biaxial strain in these studies depended on the dimension (major/minor axis ratio) of the substrate. Alternatively, a cross-shaped mold with an end-to-end length of 7.3 cm was used to create collagen gels containing dermal fibroblasts, and the two axes/arms were subjected to different amounts of stretch. This resulted in uniaxial strain in the arms and anisotropic biaxial strain in the overlap of the two arms of the cross-shaped tissue.[4] While these bioreactors have advanced cardiovascular research tremendously, a better control on the magnitude and frequency of cyclic stretch in the radial and circumferential directions is necessary for culturing aortic valves and engineered

tissues *in vitro*. Furthermore, improvements in space utilization will allow multiple tissues to be cultured simultaneously and save time. This paper describes our design of a novel biaxial stretch bioreactor with utility in both mechanobiology studies and tissue engineering applications.

The behavior of aortic valves under physiological flow is strongly related to their mechanical/structural properties, which are mainly governed by the ECM fiber architecture.[1] The mechanical properties, such as the stress-strain curve of healthy aortic cusps under uniaxial or biaxial stretch have been extensively studied[17]. Their general deformation models *in vivo* were developed based on ultrasound and computed tomography techniques.[3, 23] Recent studies tracked the deformations of a set of markers on the cusps during stretch *in vitro*, and suggested a distinct mechanical behavior on different sections (free edge, middle, and root area) of the aortic cusps.[8, 42] In terms of heterogeneous local ECM architecture, however, only the alignment and branching patterns of collagen fibers in the cusps have been mearsured.[33] In this study, detailed local deformation and strain maps of entire aortic cusps under biaxial stretch with better resolution were acquired. This knowledge will provide insights on the anisotropic and heterogeneous structure of native valves and assist in improved tissue-engineered valve design.

We have designed a novel bioreactor to culture tissue segments based on three main criteria: 1) achieve independent and controllable biaxial stretch in both radial

and circumferential directions; 2) capture images of cusps under biaxial stretch for detailed strain field analysis; 3) isolate chambers to avoid any chemical interference among the samples during culture. The custom bioreactor was validated for its capacity to maintain sterility and tissue phenotype during a 14-day culture within an incubator. We also report differences in the strain patterns and main ECM protein contents of freshly isolated aortic valve cusps (fibrosa vs. ventricularis and left vs. right vs. noncoronary cusps) and those cultured within the bioreactor for 14 days.

Materials and Methods

Design and fabrication of the bioreactor

The custom bioreactor is comprised of four modularized systems: 1) an actuating system to provide designed stretch and flexure; 2) a control system to precisely control the loading profiles; 3) four isolated culture chambers to maintain sterility and provide cell/tissue culture environment; and 4) an image capture system to collect data for digital image correlation (DIC) analysis. The bioreactor has a small footprint to fit entirely inside an incubator, as shown in Figure 9. The modular design also eases the maintenance and allows flexibility for future modifications, such as culturing cell-seeded silicone membranes and tissue-engineered heart valves. The culture chambers provide enough space for 25% elongations in both radial and circumferential directions for specimens with size up to 25mm × 20mm.

In this study, specimens were mounted using stainless steel hooks (MAX Co. ltd., Japan) along the perimeters. One side of the specimen was mounted on a fixed rod, while the other three sides were mounted on sliding rods connected to actuator arms along two directions via motion transfer parts. The positions of these parts are adjustable along the actuator arms to fit samples with different sizes. The hooks are movable along the rods to minimize the sliding friction and distortion of biaxial stretch. As the four chambers are parallel to each other, the actuator arms can be simultaneously driven by three linear actuators (Haydon Kerk Motion Solutions, Inc., Waterbury, CT), one radial and two circumferential. The linear actuator contains a stepper motor, a lead screw, and an attached nut that connects to an actuator arm. The lead screw and nut assembly transform rotation into linear motion along the lead screw, which can reach a 0.008 mm/step linear displacement. The stepper motor can generate large torque output with stable rotation of 1.8 degrees in each step, which enables a control system with high precision using a step-by-step control scheme. The profile of stretch is controlled by changing the duration between each step via software developed in the LabVIEW environment (National Instruments Corp., Austin, TX). The control system is equipped with a USB-based data acquisition/control board (National Instruments Corp.), which is suitable for digital Transistor–transistor logic (TTL) signal acquisition and generation through USB interface on a PC. The accuracy of the control can be verified by DIC analysis in which the image is captured by a

digital microscope camera with a macro photography lens (Moticam, Motic North America, Canada) to capture the positions of markers on the specimens.

The materials used in culture chambers are all biocompatible, corrosion-resistant, and suitable for sterilization. As optical transparency is preferred for macroscopic observation, the culture chambers are 3D printed using acrylic (PMMA), which makes them completely transparent and stable under repeated UV sterilization. The motion transfer parts that connect the hooks along the specimens and the actuator arms are fabricated by a computer numeric control machine from 316L stainless steel in Proto Labs, Inc., NC. The customized actuator arms are milled from 316L stainless steel by Misumi, Inc., Japan. The sterile bioreactor components were assembled in a laminar flow hood.

Digital image correlation analysis

DIC is a powerful tool used to evaluate the deformation of a sample by comparing changes in a marker field on an original sample vs. a deformed sample. Since this methodology is based on the grayscale values of pixels in a digital image, DIC offers strain analysis with high precision compared to traditional methods. To accurately track the markers, the marker field must have a non-repetitive and high-contrast pattern. Depending on the size of a sample, usually either a paint sprayer or an airbrush is used to generate a random marker field.[20] In our study, a dark-colored, fast-drying paint (McMaster-Carr Corporation, Atlanta, GA) was sprayed on the sample surface after it was cleaned with 70% alcohol and air-dried to enhance the stability and reduce the drying time of the paint. The digital images of

specimens under original and stretched conditions were captured and imported into an analyzing software (Ncorr v1.2, GA). The magnitude of stretch was verified by the elongation rate calculated based on the dimensions of deformed/original interested area on images. The displacement and strain fields were also generated for further analysis. Table 1 shows the various conditions where DIC was applied to verify stretch magnitude and analyze strain patterns.

Validation of controlled biaxial stretch

A piece of silicone rubber membrane was tested to verify the device's ability to apply independently controlled biaxial stretch and the feasibility of DIC. The displacement and strain fields of the specimen were obtained under three stretch conditions shown in Table 1. The results were compared to simulation results generated by finite element method using MSC Nastran software (MSC Software Corporation, Newport Beach, CA), which determined the patterns of strain fields under an ideal condition. The dimensions of the specimen were set at 25mm × 20mm × 0.5mm. Elastic modulus of the silicone rubber was 2.5 Mp; Poisson's ratio was 0.48 and density was 1g/cm^2. The specimen was subjected to a four-edge stretch with a 1-mm interval between loading points.

Measuring strain patterns of coronary and noncoronary cusps

We measured the strain patterns of freshly isolated coronary vs. noncoronary and fibrosa vs. ventricularis sides of the cusps under stretch. Pig hearts were collected from a local slaughterhouse (Wampler's Farm Sausage, Lenoir City, TN). The left,

right, and noncoronary cusps were isolated and washed twice with phosphate-buffered saline (PBS). Flexible sterile silicone membranes (Flexcell International Corporation, Burlington, NC) were cut into identical size (25mm × 20mm), drilled with guiding holes along four edges for mounting, and lined under the aortic tissues to offer necessary support.[1, 4, 6] The cusps were trimmed into the same size as the silicone membranes and were mounted together to ensure identical testing area and stretch ratio for all the samples.

Digital images of original and deformed cusps were taken with applied random marker fields, as previously mentioned. Both displacement and strain fields were obtained through DIC, where three stretch conditions were tested as described in Table 1. For each cusp, strain fields on both fibrosa and ventricularis sides were analyzed to gain insights on the layered ECM structure since the components and mechanical properties of the three layers are remarkably different. The concentrations of ECM components in the three cusps were also measured through collagen and glycosaminoglycan (GAG) assays. The study was repeated with three different aortic valves.

Cyclic stretch conditioning

To verify the device's ability to condition multiple specimens under cyclic stretch, four porcine aortic valve cusps isolated from four different hearts were cultured in the bioreactor for 14 days with media changed every two days. For each heart, one coronary cusp was cultured under a cyclic biaxial stretch: elongations along

radial and circumferential directions were 15% and 10%, respectively with a frequency of 0.3 Hz. The other coronary cusp was cultured under static condition in 5-ml culture media [Dulbecco's modified eagles medium (DMEM) supplemented with 10% bovine growth serum (BGS) and 1% antibiotic, all purchased from Mediatech Inc.] in 6-well plates at 37°C, 5% CO_2 for 14 days. After conditioning, DIC was used to obtain the strain patterns of the cultured samples, followed by collagen and GAG assays to determine remodeling of the ECM structure.

Hematoxylin & Eosin (H&E) staining, DNA, collagen and GAG assays

Paraffin embedded and sectioned tissues were stained with Hematoxylin (Electron Microscopy Sciences, PA) and Eosin Y (Fisher Scientific) to visualize cell distribution within the tissues using established histology procedure.[27] The stained sections were imaged using a brightfield microscope. Collagen and GAG contents were measured as described previously.[27] Briefly, the wet tissues were lyophilized, then digested in Proteinase-K solution (1 mg/ml) (Sigma) at 63°C for 12 hours in a water bath. After sonication, DNA, collagen and GAG were tagged with Hoechst 33258 dye (Sigma), direct 80 sirius red dye (Tokyo chemical industry co., Ltd, Tokyo, Japan) and dimethylmethylene blue dye (Sigma) respectively. The fluorescence emissions were measured using a BioTek Synergy H1 fluorocolorimeter at 458, 540, and 525nm respectively. Calf thymus DNA standards (Sigma) were used to calculate the DNA density. Collagen from calf skin standards (Fisher) and chondroitin sulfate glycosaminoglycan standards (Sigma)

were used to calculate collagen and GAG concentrations respectively. The results were normalized to tissue dry weight or DNA content.

Maintenance of sterility

The bioreactor parts were cleaned with 10% bleach, rinsed in tap water, and wiped with 70% ethanol. The stainless steel parts were then autoclaved at 250°C for 30 minutes, and the culture chambers were placed under UV for 30 minutes on each side. All parts were then assembled inside a laminar flow hood to maintain sterility. During culture within the incubator, the sterility of the media was inspected by macroscopic observation under the microscope.

Statistical Analysis

Results are represented as means ± standard error. Statistical analysis was performed with one-way analysis of variances (ANOVA) and results were considered significant at $p \leq 0.05$. Each study was repeated with at least 3 different aortic valves (n=3).

Results

DIC results on silicone rubber membrane

The term “strain” is defined as the ratio of change in length to original length. Under different biaxial stretch conditions, the strain distributions retained the same patterns: the normal and shear strain distributed relatively evenly on majority of the

substrate, except for the area around hooks, where the gradient was higher. The medians of the normal strain along radial direction were 0.047, 0.102 and 0.151. The medians of the normal strain along circumferential direction were 0.104, 0.101 and 0.097. The medians of shear strains remained less than 0.01.

Finite element analysis

The strain fields generated from simulation also showed patterns similar to the experimental results, as shown in Figure 10. They were distributed relatively evenly in the central area while the strain had larger gradient on the boundaries. The shear strain was 0 except for the four corners. The figure shows deformation and strain fields under biaxial stretch with universal elongations of 5% and 15% along the radial and circumferential directions, respectively.

Strain fields on fresh aortic valve cusps

Similar to the strain fields on the silicone rubber membrane, the strain fields on aortic valve cusps retained distinct patterns under different levels of stretch. As shown in Figure 11, the contour maps of the strain, the positions of the contour lines had only trivial changes while the values of strain increased as the tissue was elongated. For all cusps, the radial strain fields on the fibrosa side were more heterogeneous compared to the ventricularis side, as shown in Figure 12. The strain fields on the fibrosa side were also very sensitive to the distribution of thick collagen fibers. Therefore, to limit variability, the ventricularis side was selected for measuring radial strain field for each cusp. Figure 13 shows radial strain fields of

three cusps from the same aortic valve under biaxial elongations of 15% and 10% along the radial and circumferential directions, respectively. The radial stain in the left and right cusps was significantly smaller near the free edge than the middle and root areas. This pattern was distinct in the coronary cusps but not so obvious in the noncoronary cusps, where distribution of strain was relatively even on the entire cusps, as shown in Figure 14.

Strain fields on stretched cusps and controls

The radial strain patterns observed in fresh coronary cusps were still discernible in the stretched coronary cusps; however, the differences in radial stain between free edge and middle or root were smaller compared to fresh controls. In the static control groups, the strain distributed relatively evenly in most areas of each cusp, which suggested significant ECM remodeling/degradation during the static culture.

Collagen and GAG contents in stretched cusps and controls

For fresh tissues, as we have previously reported,[27] no significant difference was observed between the coronary and noncoronary cusps for wet weight to dry weight ratio, collagen, and GAG content. We found that the wet weight to dry weight ratio of the static control tissues was significantly lower than stretched and fresh tissues. Similarly, the GAG content of the static controls was significantly greater than the fresh group, as shown in Figure 15. There was no significant difference in collagen content normalized to dry weight for the three groups; however, the total collagen content was 18.1% higher in the stretched tissues than

the other two groups. Similarly, collagen contents normalized to DNA was significantly greater in the stretch group than in the other two groups. H&E staining showed that denudation occurred on the cusp surface facing the silicone membrane (Figure 16). Additionally, increased cell number was observed on the top surface that was in contact with the media.

Discussion

In this manuscript, we developed a novel biaxial tissue culture bioreactor for aortic valves that can apply precisely controlled strain in both radial and circumferential directions. Our design is an improvement over existing designs in three aspects: 1) we used a stepper-motor-based actuating system to precisely control the magnitude and frequency of the cyclic biaxial stretch, which is a necessity to mimic the native stretch environment of aortic valve cusps; 2) by applying randomly distributed markers at a high density, we obtained detailed strain fields of the deformed cusps using DIC, which then enabled us to analyze the heterogeneous structural properties of aortic cusps on a microscale; and 3) using four isolated chambers, we can culture multiple samples under different culture media while keeping the stretch condition identical. We first validated the bioreactor's ability to apply designed biaxial stretch by DIC and DIC's ability to generate accurate deformation and strain fields by comparing results obtained from a silicone rubber membrane to the finite element method. Furthermore, we report that biaxial stretch better maintains native ECM proteins and structure for aortic valves compared to

static controls. The biaxial stretch to validate this bioreactor was selected to be 10% circumferential and 15% radial strain. The reported tensile strains for aortic valves ranges from 9% to 11% (circumferential) and 13% to 35% (radial). The radial strain varies widely from systole to diastole, regionally within the valve (middle, root, etc.) and also changes with age and diseased conditions.[7, 40, 42] Therefore, to keep the experimental conditions manageable, we selected 15% radial strain as a representative systolic stretch for this validation study.[3] The frequency of 0.3 Hz was also representative of those used to condition engineered valves, which often range from 0.03 to 0.5 Hz.[18, 28, 34] The actuator arms can reach a stable linear speed of 16mm/s, corresponding to 1.28 Hz for 15% stretch, which fulfills the demand to apply cyclic stretch at a physiological frequency for cardiovascular tissues (1.167 Hz).[6] Using DIC, we also observed distinct strain patterns on the fibrosa and ventricularis sides and among the three cusps in a fresh aortic valve.

Validation of the stretch

During the 14-day culture period, no contamination was observed, which verified the customized bioreactor's ability to maintain a sterile environment while applying cyclic biaxial stretch on the tissues. In order to produce adequate strain uniformity, we used six and four hooks along circumferential and radial directions, respectively.[9, 36] During stretch, the hooks slid smoothly and adjusted their positions as the samples deformed, thus delivering biaxial stretch effectively and evenly to the samples. The uniform strain fields formed on an isotropic material

(silicone rubber) are shown in Fig. 10, where the hooks only affected the edges of the strain fields. In addition to tissues, our custom bioreactor can easily be modified for cells on a flexible substrate and engineered tissues for both mechanobiology and tissue engineering applications.

Biaxial stretch improved maintenance of native ECM structure

Table 2 shows strain patterns of tissues from the fresh, stretch and static groups after 14 days of culture under the condition described in Table 1. With a similar average strain of around 0.15, the standard deviations of the fresh and stretch groups were 103.8% and 34.6% more respectively than the static group, which suggests that strain distribution in the static control was relatively homogeneous on the entire tissue. In fresh cusps, the free edge areas that contribute to valve coaptation generally experienced small radial strains (less than 0.1). These coaptation areas were comparable in the fresh and stretch groups; however, it reduced by 55.6% in the static group. We hypothesize that this ECM remodeling in the static group may alter the mechanical environment and lead to improper sealing of the aorta as the valve closes.

Previous studies have shown that strain field anisotropy is an independent regulator of cell phenotype and matrix remodeling in soft tissues.[13] Balachandran et al. have reported that compared to fresh control, collagen content was significantly decreased in aortic valve tissues cultured under 10% uniaxial cyclic stretch along circumferential direction.[6] According to Huang et al., engineered

artery tissues under biaxial stretch remodeled collagen fibers and showed distinctive feature of undulation and crimp, which was more native-like organization that was absent in both uniaxial and static groups. These tissues also had increased mechanical strength and compliance compared to uniaxial and static groups due to a more physiological collagen fiber structure and matrix orientation.[18] In this study, we observed significantly increased collagen content normalized to DNA in the biaxial stretch group. This suggests that biaxial stretch promoted collagen synthesis to maintain the ECM as compared to static culture. Additionally, the increased GAG content in the static group also undermine the tissues' mechanical properties, since tissues with higher concentration of GAGs has lower stiffness under stretch.[2, 14, 31] Since GAGs can retain large amounts of water, excessive GAGs result in dramatically increased tissue thickness and reduced structural organization, which is commonly found in aged and diseased heart valves.[14, 22] Accordingly, the significantly higher GAG content and lower dry-to-wet weight ratio in static cultures than in the fresh tissues suggest the abnormal ECM degradation or remodeling under static culture.

Distinct strain patterns of fresh aortic valve cusps

A major cause of tissue-engineered aortic valve failure is thought to be the engineered valve's inability to mimic the anisotropic and heterogeneous ECM structure of native tissues. It is well known that cell characteristics and ECM composition is different between the fibrosa and ventricularis sides[29], where the calcific aortic valve disease frequently exists on the fibrosa side[44]. Similarly,

heterogeneity in the collagen fibers has been reported among the aortic valve cusps.[26] Recent reports from our group have also shown that there are cellular differences between coronary and noncoronary cusps in aortic heart valves: cells within noncoronary cusps show an elevated response to pathological conditions.[27] However, the exact mechanisms of the function of native valves and pathology of calcific valve disease are still under investigation. The detailed deformation and strain fields generated through DIC would thus be valuable for tissue engineering and help mimic the mechanical/structural properties of native tissues. We studied how the strain fields on the fibrosa and ventricularis sides and on the left, right, and noncoronary cusps vary to better understand the micromechanical environment that contribute to the unique cellular characteristics within the cusps.

We observed that, in general, because of the alignment of collagen and elastin fibers, the radial strain fields were more heterogeneous than the circumferential and shear strain fields. Note that the majority of the thick collagen fibers in aortic valves are aligned along the circumferential direction. We also observed that, during stretch, the areas in between the fibers deformed first in the radial direction, causing larger strain in these areas than in areas where the fibers are located. The heterogeneity was more obvious on the fibrosa side, since the thick collagen fibers are distributed primarily on this side, while the GAG and elastin sheets under the collagen fibers reduces the heterogeneity on the ventricularis side. The retention of strain patterns under different levels of stretch indicated that the integrity of the

tissues as the relative position of ECM fibers remained unchanged. Interestingly, the complex ECM composition in valve tissues induced an anisotropic structure resulting in a non-zero shear strain under uniform biaxial stretch. The strain patterns of the three cusps in an aortic valve were distinct, which suggested unique distribution of ECM fibers in these cusps.

The strain distribution for the left cusp was asymmetric, whereas the strain fields of right and noncoronary cusps were relatively symmetric. This supports the asymmetric distribution of collagen fibers in the left cusp.[26, 33] According to Doehring et al., the collagen bundles on the left side of left cusps were much thicker than on the right side, forming a more even distribution on the right side. For right and noncoronary cusps, the collagen bundles were relatively symmetric, although thicker in the right cusps.[5] The strain near the free edges of the coronary cusps was significantly smaller than in other areas, which contributed to formation of a large coaptation area that ensured seal of the aorta.[16]

Limitations and future works

This study employed DIC to study the normal and shear strain magnitudes and could not determine the principal directions of the strain in different regions of the cusp. Since DIC uses pixels of a digital image instead of manually divided sections as used in traditional methods, additional computer programs would be needed for obtaining the principal directions onto the strain fields generated by DIC and will

be investigated in future work. Furthermore, since DIC was used to measure the deformation of the tissue, they required support from silicone membranes to be free of deformation before stretch. Without the silicone linings, the highly flexible cusps were either stretched or bended by gravity. Silicone linings are commonly used as a supporting material for tissue-engineered constructs.[35, 43] Addition of the silicone lining increased the total stretch forces required to pull both the cusp and lining. However, if the deformation of a cusp is maintained, the forces experienced by the cusp should be identical as it is mainly determined by the cusp stiffness, which is an inherent property. Additionally, a 2-week culture period was used in this study to compare our results to published mechanobiology studies. A longer culture period may be needed for developing tissue-engineered valve products and will be studied in future. Furthermore, as is observed for tissue-engineered constructs under cyclic stretch[30, 37], the cusp surface in contact with the lining experienced some denudation. The larger cell accumulation on the top surface is due to limited diffusion of culture media, which is a well-documented limitation for bioreactor devices (Figure 16).[21, 34, 41] While this should not influence the strain profile reported in this study, any effect on cell distribution and ECM components will be evaluated in future.

Conclusions

In conclusion, our custom bioreactor is capable of applying controllable cyclic biaxial stretch on aortic valve tissues. Biaxial stretch maintained native anisotropy

and proteins during two week's culture better than static controls. Furthermore, DIC is a powerful tool for gaining insight into the micro ECM structure in aortic valves by providing detailed deformation and strain fields. The heterogeneous ECM structure in aortic valves is critical in sealing the aorta under a physiological environment. Therefore, to design long-lasting and properly functioning tissue-engineered heart valves, it is critical to more accurately mimic the heterogeneity of the mechanical properties and ECM structure of native valves.

Acknowledgements

This study was supported by National Science Foundation BRIGE award no. EEC-1342189.

References

1. Billiar K. L. and M. S. Sacks. Biaxial mechanical properties of the natural and glutaraldehyde treated aortic valve cusp--Part I: Experimental results. J Biomech Eng 122:23-30, 2000.
2. Lovekamp J. J., D. T. Simionescu, J. J. Mercuri, B. Zubiate, M. S. Sacks and N. R. Vyavahare. Stability and function of glycosaminoglycans in porcine bioprosthetic heart valves. Biomaterials 27:1507-1518,2006.
3. Aggarwal A., A. M. Pouch, E. Lai, J. Lesicko, P. A. Yushkevich, J. H. Gorman Iii, R. C. Gorman and M. S. Sacks. In-vivo heterogeneous functional and residual strains in human aortic valve leaflets. *J Biomech* 49: 2481-2490, 2016.
4. Bai Y., P. F. Lee, J. D. Humphrey and A. T. Yeh. Sequential multimodal microscopic imaging and biaxial mechanical testing of living multicomponent tissue constructs. *Ann Biomed Eng* 42: 1791-1805, 2014.
5. Balachandran K., S. Konduri, P. Sucosky, H. Jo and A. P. Yoganathan. An ex vivo study of the biological properties of porcine aortic valves in response to circumferential cyclic stretch. *Ann Biomed Eng* 34: 1655-1665, 2006.
6. Balachandran K., P. Sucosky, H. Jo and A. P. Yoganathan. Elevated cyclic stretch alters matrix remodeling in aortic valve cusps: implications for degenerative aortic valve disease. *Am J Physiol Heart Circ Physiol* 296: H756-764, 2009.
7. Balachandran K., P. Sucosky and A. P. Yoganathan. Hemodynamics and mechanobiology of aortic valve inflammation and calcification. *Int J Inflam* 2011: 263870, 2011.
8. Doehring T. C., M. Kahelin and I. Vesely. Direct measurement of nonuniform large deformations in soft tissues during uniaxial extension. *J Biomech Eng* 131: 061001, 2009.
9. Eilaghi A., J. G. Flanagan, G. W. Brodland and C. R. Ethier. Strain uniformity in biaxial specimens is highly sensitive to attachment details. *J Biomech Eng* 131: 091003, 2009.

10. Engelmayr G. C., D. K. Hildebrand, F. W. H. Sutherland, J. E. Mayer and M. S. Sacks. A novel bioreactor for the dynamic flexural stimulation of tissue engineered heart valve biomaterials. *Biomaterials* 24: 2523-2532, 2003.

11. Engelmayr G. C., Jr., L. Soletti, S. C. Vigmostad, S. G. Budilarto, W. J. Federspiel, K. B. Chandran, D. A. Vorp and M. S. Sacks. A novel flex-stretch-flow bioreactor for the study of engineered heart valve tissue mechanobiology. *Ann Biomed Eng* 36: 700-712, 2008.

12. Fisher C. I., J. Chen and W. D. Merryman. Calcific nodule morphogenesis by heart valve interstitial cells is strain dependent. Biomech Model Mechanobiol 12:5-17, 2013.

13. Gould R. A., K. Chin, T. P. Santisakultarm, A. Dropkin, J. M. Richards, C. B. Schaffer and J. T. Butcher. Cyclic strain anisotropy regulates valvular interstitial cell phenotype and tissue remodeling in three-dimensional culture. *Acta Biomater* 8: 1710-1719, 2012.

14. Gould R. A., R. Sinha, H. Aziz, R. Rouf, H. C. Dietz, 3rd, D. P. Judge and J. Butcher. Multi-scale biomechanical remodeling in aging and genetic mutant murine mitral valve leaflets: insights into Marfan syndrome. *PLoS One* 7: e44639, 2012.

15. Gupta V., J. A. Werdenberg, B. D. Lawrence, J. S. Mendez, E. H. Stephens and K. J. Grande-Allen. Reversible secretion of glycosaminoglycans and proteoglycans by cyclically stretched valvular cells in 3D culture. *Ann Biomed Eng* 36: 1092-1103, 2008.

16. Hammer P. E., C. A. Pacak, R. D. Howe and P. J. del Nido. Straightening of curved pattern of collagen fibers under load controls aortic valve shape. *J Biomech* 47: 341-346, 2014.

17. Hasan A., K. Ragaert, W. Swieszkowski, S. Selimovic, A. Paul, G. Camci-Unal, M. R. Mofrad and A. Khademhosseini. Biomechanical properties of native and tissue engineered heart valve constructs. *J Biomech* 47: 1949-1963, 2014.

18. Huang A. H., J. L. Balestrini, B. V. Udelsman, K. C. Zhou, L. Zhao, J. Ferruzzi, B. C. Starcher, M. J. Levene, J. D. Humphrey and L. E. Niklason. Biaxial

Stretch Improves Elastic Fiber Maturation, Collagen Arrangement, and Mechanical Properties in Engineered Arteries. *Tissue Eng Part C Methods* 22: 524-533, 2016.

19. Huang S. and H. Y. Huang. Biaxial stress relaxation of semilunar heart valve leaflets during simulated collagen catabolism: Effects of collagenase concentration and equibiaxial strain state. *Proc Inst Mech Eng H* 229: 721-731, 2015.

20. Justin Blaber A. A. http://www.ncorr.com/index.php/contact.

21. Kensah G., I. Gruh, J. Viering, H. Schumann, J. Dahlmann, H. Meyer, D. Skvorc, A. Bar, P. Akhyari, A. Heisterkamp, A. Haverich and U. Martin. A novel miniaturized multimodal bioreactor for continuous in situ assessment of bioartificial cardiac tissue during stimulation and maturation. *Tissue Eng Part C Methods* 17: 463-473, 2011.

22. Krishnamurthy V. K., F. Guilak, D. A. Narmoneva and R. B. Hinton. Regional structure-function relationships in mouse aortic valve tissue. *J Biomech* 44: 77-83, 2011.

23. Kulp S., Z. Qian, M. Vannan, S. Rinehart and D. Metaxas. Patient-specific aortic valve blood flow simulations. In: *2014 IEEE 11th International Symposium on Biomedical Imaging (ISBI)*2014, p. 939-942.

24. Lehmann S., T. Walther, J. Kempfert, A. Rastan, J. Garbade, S. Dhein and F. W. Mohr. Mechanical strain and the aortic valve: influence on fibroblasts, extracellular matrix, and potential stenosis. *Ann Thorac Surg* 88: 1476-1483, 2009.

25. Lei Y. and Z. Ferdous. Design considerations and challenges for mechanical stretch bioreactors in tissue engineering. Biotechnol Prog 32:543-553, 2016.

26. Marom G., M. Peleg, R. Halevi, M. Rosenfeld, E. Raanani, A. Hamdan and R. Haj-Ali. Fluid-structure interaction model of aortic valve with porcine-specific collagen fiber alignment in the cusps. *J Biomech Eng* 135: 101001-101006, 2013.

27. Masjedi S., A. Amarnath, K. M. Baily and Z. Ferdous. Comparison of calcification potential of valvular interstitial cells isolated from individual aortic valve cusps. *Cardiovasc Pathol* 25: 185-194, 2016.

28. Masoumi N., M. C. Howell, K. L. Johnson, M. J. Niesslein, G. Gerber and G. C. Engelmayr, Jr. Design and testing of a cyclic stretch and flexure bioreactor for evaluating engineered heart valve tissues based on poly(glycerol sebacate) scaffolds. *Proc Inst Mech Eng H* 228: 576-586, 2014.

29. Miura K. A. O. and H. Katoh. Structural and Histochemical Alterations in the Aortic Valves of Elderly Patients: A Comparative Study of Aortic Stenosis, Aortic Regurgitation, and Normal Valves. Biomed Res Int 2016:6125204, 2016.

30. Mundargi R., D. Venkataraman, S. Kumar, V. Mogal, R. Ortiz, J. Loo, S. Venkatraman and T. Steele. Novel Sensor-Enabled Ex Vivo Bioreactor: A New Approach towards Physiological Parameters and Porcine Artery Viability. *Biomed Res Int* 2015: 958170, 2015.

31. Naveen S. V., R. E. Ahmad, W. J. Hui, A. M. Suhaeb, M. R. Murali, R. Shanmugam and T. Kamarul. Histology, glycosaminoglycan level and cartilage stiffness in monoiodoacetate-induced osteoarthritis: comparative analysis with anterior cruciate ligament transection in rat model and human osteoarthritis. *Int J Med Sci* 11: 97-105, 2014.

32. Ramaswamy S., S. M. Boronyak, T. Le, A. Holmes, F. Sotiropoulos and M. S. Sacks. A novel bioreactor for mechanobiological studies of engineered heart valve tissue formation under pulmonary arterial physiological flow conditions. *J Biomech Eng* 136: 121009, 2014.

33. Rock C. A., L. Han and T. C. Doehring. Complex collagen fiber and membrane morphologies of the whole porcine aortic valve. *PLoS One* 9: e86087, 2014.

34. Schmidt J. B. and R. T. Tranquillo. Cyclic Stretch and Perfusion Bioreactor for Conditioning Large Diameter Engineered Tissue Tubes. *Ann Biomed Eng* 44: 1785-1797, 2016.

35. Straussman Y. Silicone Rubber Membrane As a Support for Long-term Cultivation and Electron Microscopic Processing of Nervous Tissue. *TISSUE & CELL* 5: 691-696, 1973.

36. Sun W., M. S. Sacks and M. J. Scott. Effects of Boundary Conditions on the Estimation of the Planar Biaxial Mechanical Properties of Soft Tissues. *Journal of Biomechanical Engineering* 127: 709, 2005.

37. Syedain Z. H., J. S. Weinberg and R. T. Tranquillo. Cyclic distension of fibrin-based tissue constructs: evidence of adaptation during growth of engineered connective tissue. *Proc Natl Acad Sci U S A* 105: 6537-6542, 2008.

38. Tan W., D. Scott, D. Belchenko, H. J. Qi and L. Xiao. Development and evaluation of microdevices for studying anisotropic biaxial cyclic stretch on cells. Biomed Microdevices 10:869-882, 2008.

39. Thayer P., K. Balachandran, S. Rathan, C. H. Yap, S. Arjunon, H. Jo and A. P. Yoganathan. The effects of combined cyclic stretch and pressure on the aortic valve interstitial cell phenotype. *Ann Biomed Eng* 39: 1654-1667, 2011.

40. van Geemen D., A. L. Soares, P. J. Oomen, A. Driessen-Mol, M. W. Janssen-van den Broek, A. J. van den Bogaerdt, A. J. Bogers, M. J. Goumans, F. P. Baaijens and C. V. Bouten. Age-Dependent Changes in Geometry, Tissue Composition and Mechanical Properties of Fetal to Adult Cryopreserved Human Heart Valves. *PLoS One* 11: e0149020, 2016.

41. Weidenhamer N. K. and R. T. Tranquillo. Influence of cyclic mechanical stretch and tissue constraints on cellular and collagen alignment in fibroblast-derived cell sheets. *Tissue Eng Part C Methods* 19: 386-395, 2013.

42. Weiler M., C. H. Yap, K. Balachandran, M. Padala and A. P. Yoganathan. Regional analysis of dynamic deformation characteristics of native aortic valve leaflets. *J Biomech* 44: 1459-1465, 2011.

43. Xu R., Y. Bai, J. Zhao, H. Xia, Y. Kong, Z. Yao, R. Yan, X. Zhang, X. Hu, M. Liu, Q. Yang, G. Luo and J. Wu. A silicone rubber membrane with a specific pore size enhances cell proliferation and wound regeneration via the Wnt/β-catenin pathway. *J Tissue Eng Regen Med*, 2017.

44. Yabusaki K., J. D. Hutcheson, P. Vyas, S. Bertazzo, S. C. Body, M. Aikawa and E. Aikawa. Quantification of Calcified Particles in Human Valve Tissue

Reveals Asymmetry of Calcific Aortic Valve Disease Development. Front Cardiovasc Med 3:44, 2016.

45. Yap C. H., H. S. Kim, K. Balachandran, M. Weiler, R. Haj-Ali, and A. P. Yoganathan. Dynamic deformation characteristics of porcine aortic valve leaflet under normal and hypertensive conditions. Am J Physiol Heart Circ Physiol 298:H395-405, 2010.

Appendix

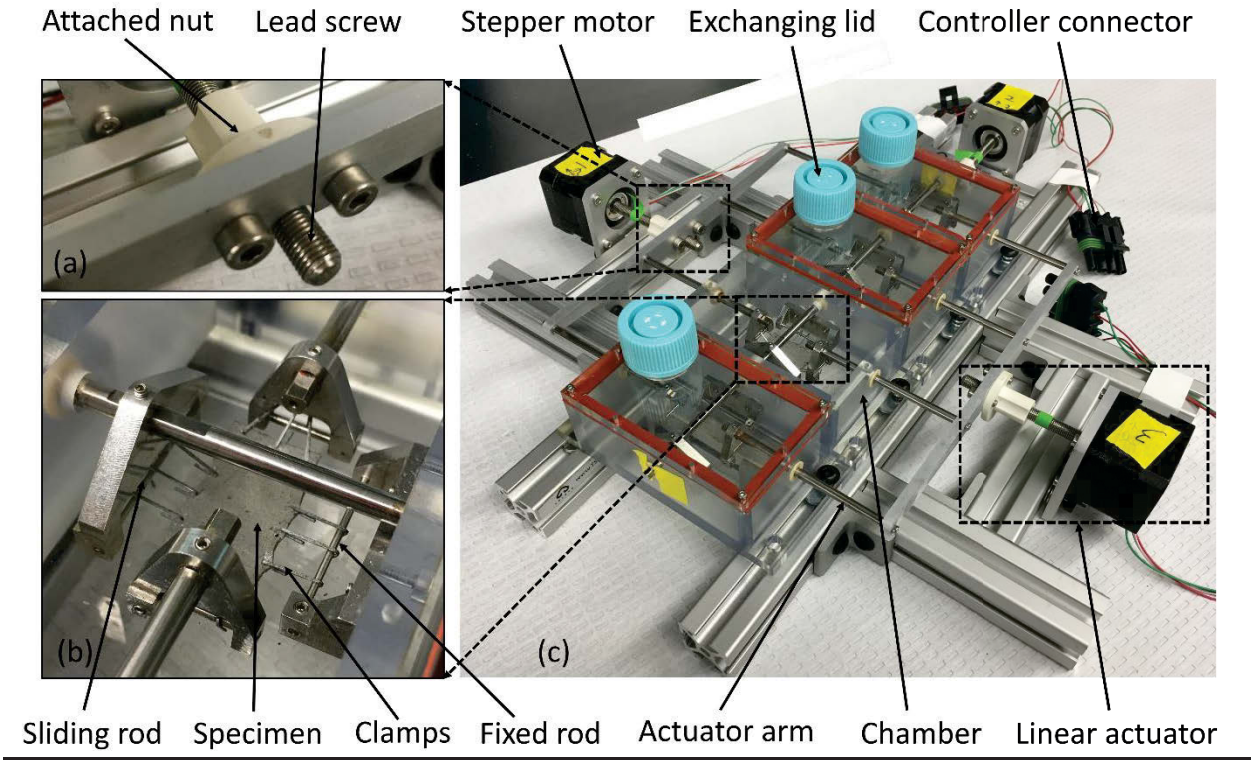


Figure 9. Layout of the custom biaxial stretch bioreactor.

(a) The linear actuator contains a lead screw-nut assembly that transforms rotation into linear motion; (b) specimen mounted using movable stainless steel hooks; (c) assembly of the biaxial stretch bioreactor with four culture chambers.

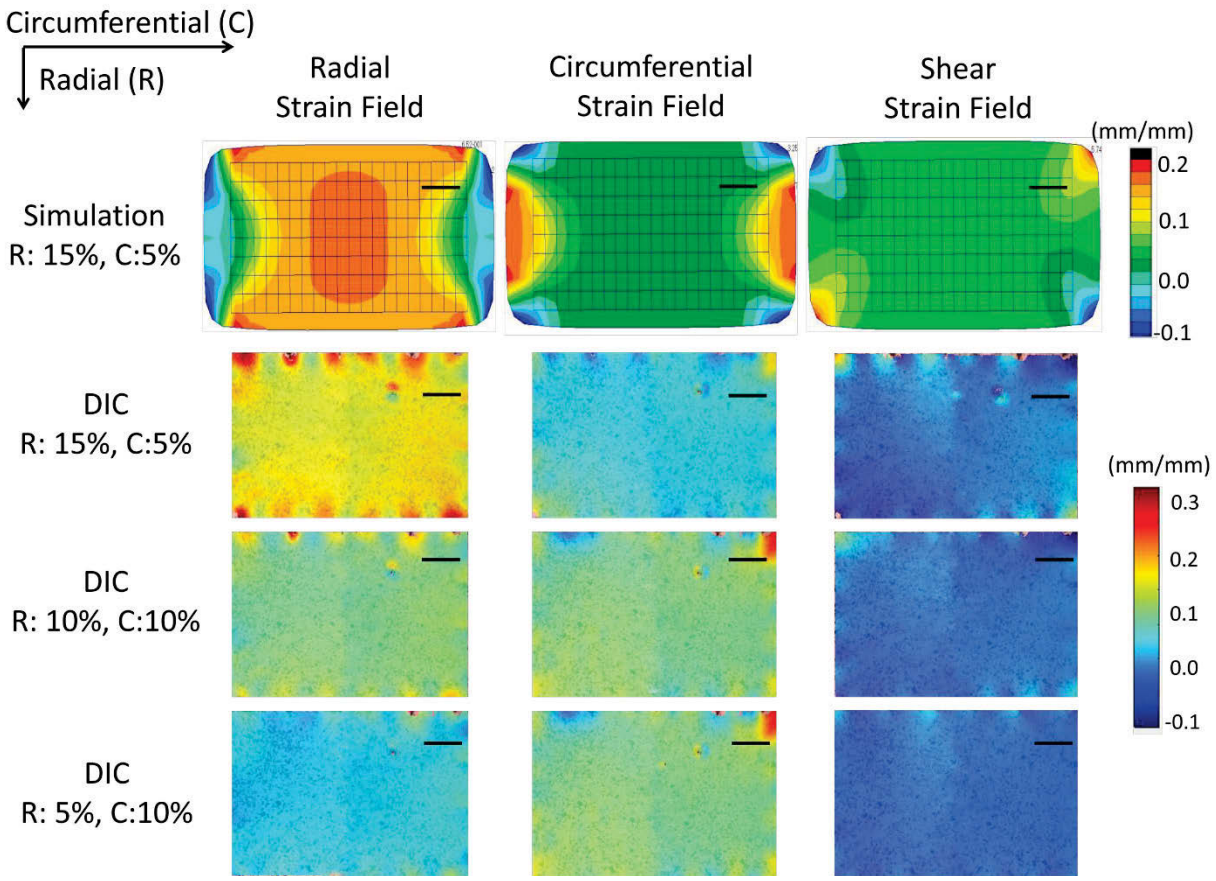


Figure 10. Radial, circumferential and shear strain

Strain fields on a silicone rubber membrane generated by simulation and DIC. Scale bars are 3mm.

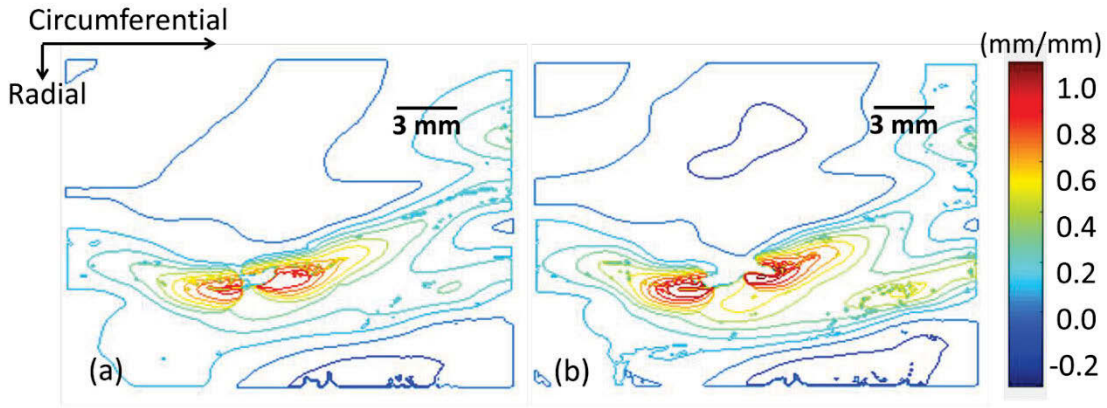


Figure 11. Strain pattern on a leaflet

Contour maps of the radial strain fields of an aortic cusp on the fibrosa side under biaxial stretch with average elongation of (a) 10%, and (b) 15 %.

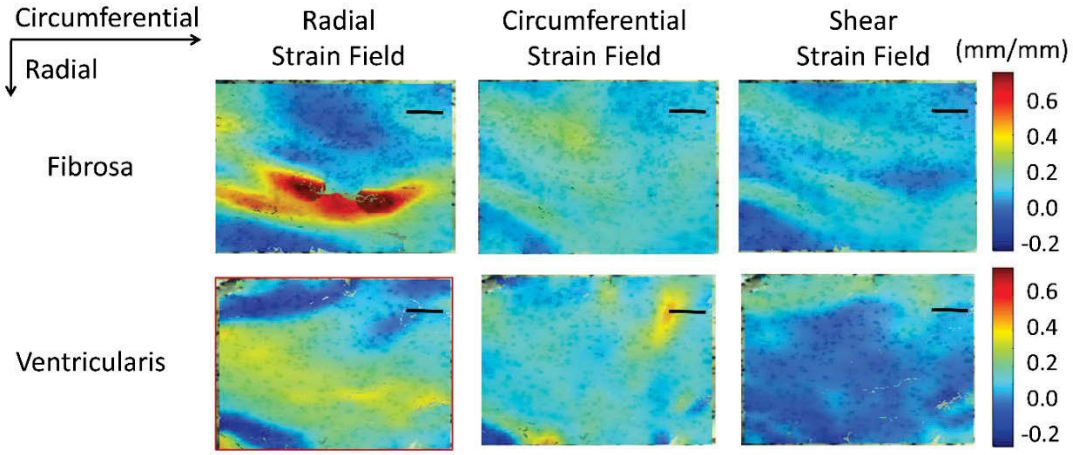


Figure 12. Strain patterns on two sides of a leaflet

Normal and shear strain patterns of a left aortic cusp on fibrosa and ventricularis sides. The radial strain on ventricularis side was selected as the characteristic strain pattern of the cusp. Scale bars are 3mm.

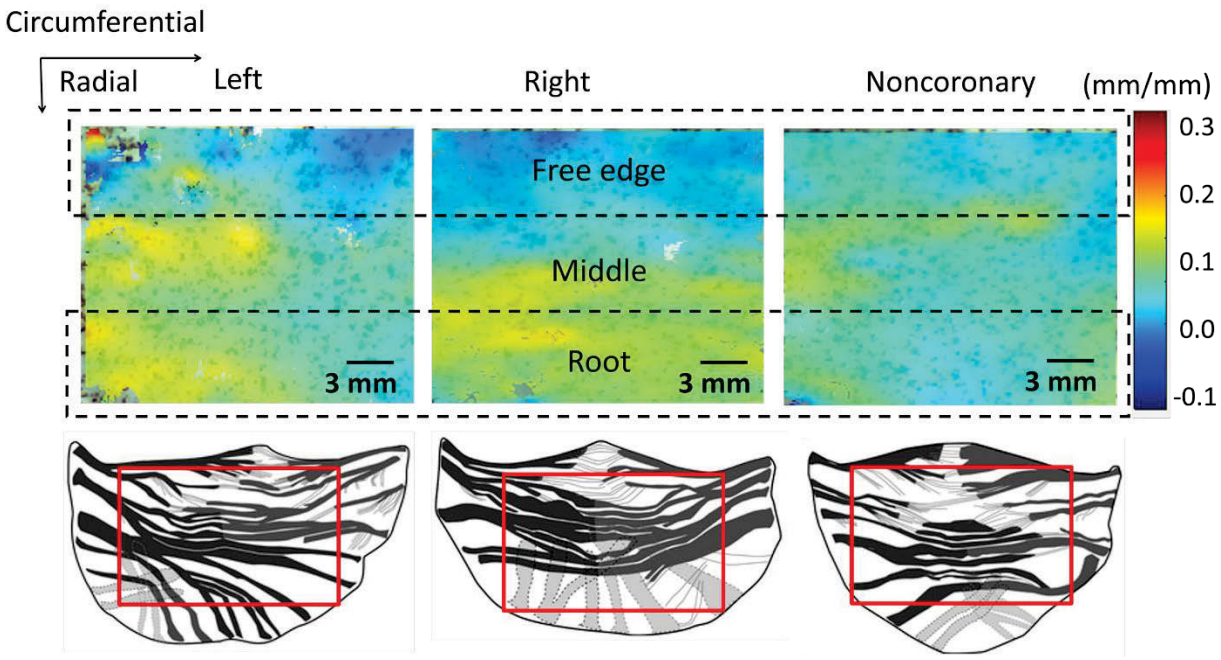


Figure 13. Strain patterns on leaflets of one valve

Characteristic strain patterns of the three aortic valve cusps (left, right, noncoronary), which correspond to the alignment of collagen fibers in three cusps reported by Doehring et al. (open access publication).

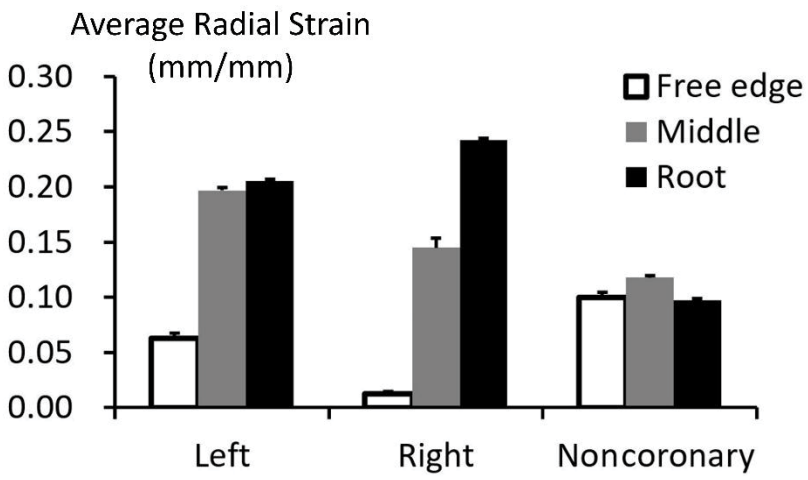


Figure 14. Strain patterns showed by average strain

Distinct strain distribution in the free edge, middle and root sections of left, right and noncoronary cusps. Figure shows average radial strain on the ventricularis side.

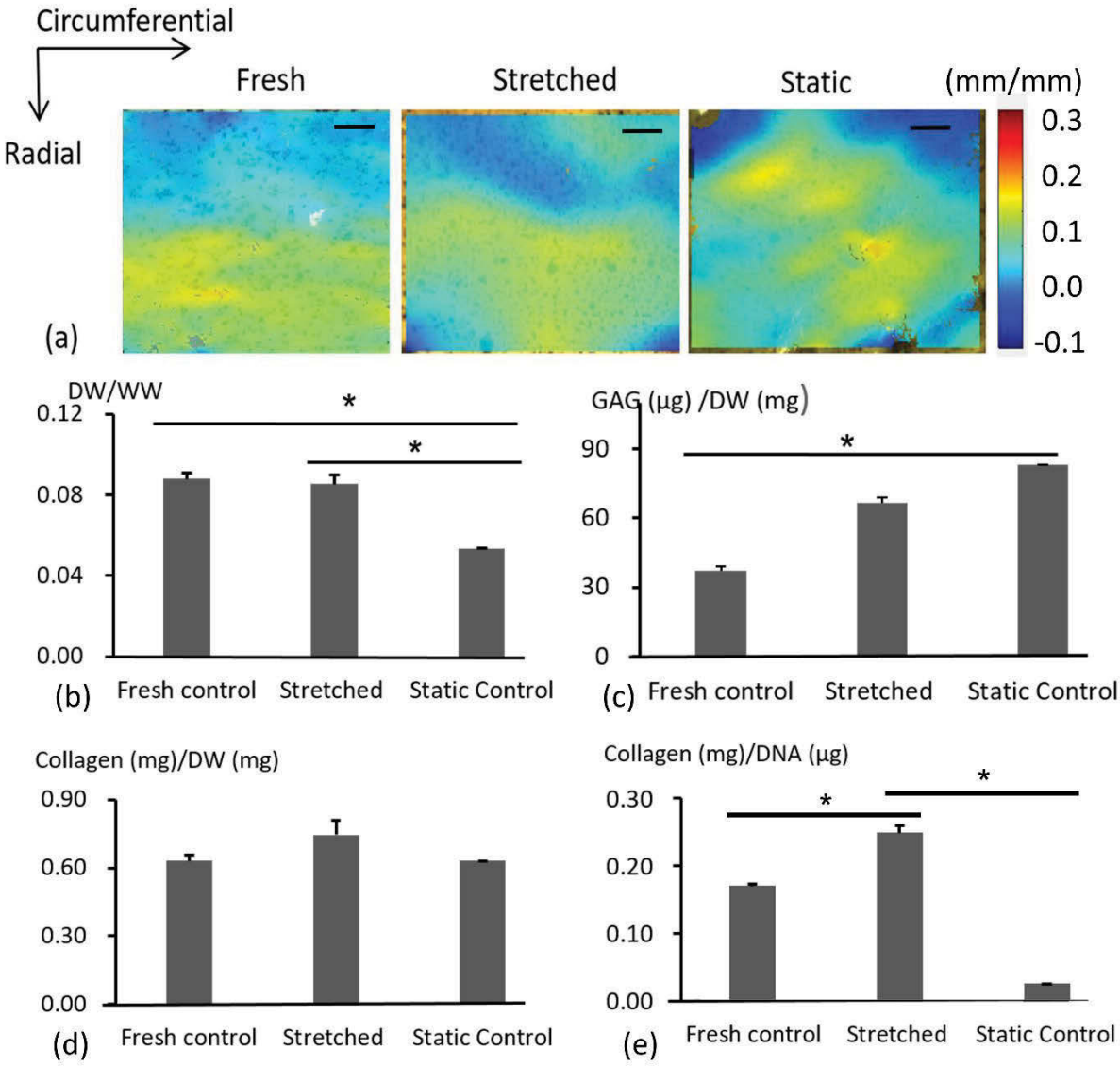


Figure 15. Results of experimental and control groups

(a) Strain patterns, (b) dry weight (DW) to wet weight (WW) ratio, (c) GAG, (d) collagen contents normalized to dry weight, and (e) collagen contents normalized to DNA in fresh control, stretched and static control groups. Scale bars are 3mm. *= $p<0.05$.

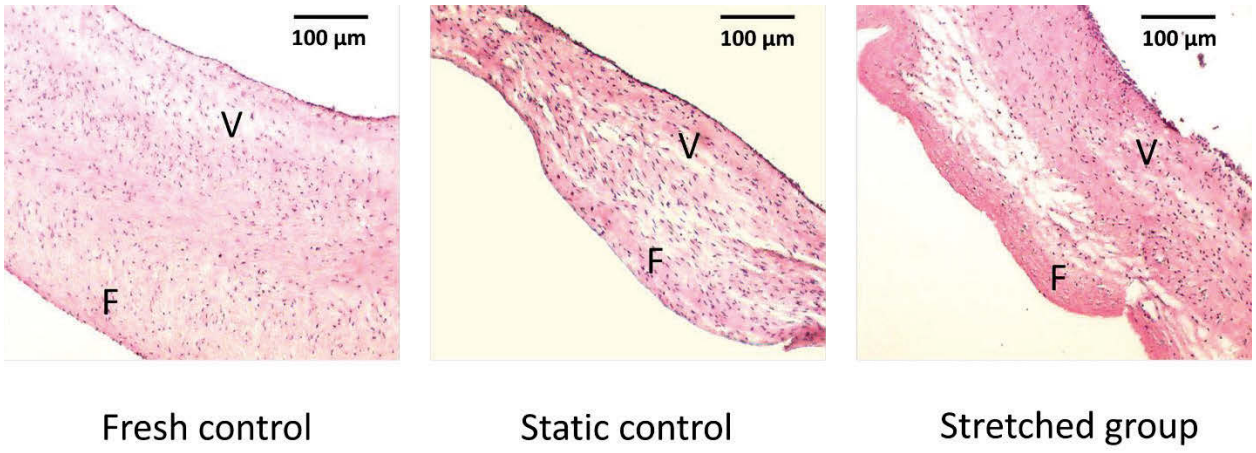


Figure 16. H&E straining of experimental and control groups

H&E staining images of cusps in fresh, static and stretched groups. Cusp surface in contact with the lining experienced some denudation (fibrosa side), while cells accumulated on the top surface (ventricularis side) due to limited diffusion of culture media.

CHAPTER III
A LAYERED AND HETEROGENEOUS FINITE ELEMENT MODEL FOR MECHANOBIOLOGICALSIMULATION OF AORTIC VALVES

Abstract

Aortic valve disease (AVD) is a major cardiovascular disorder that affects about 25% of the elderly population. Finite element (FE) analysis has widely been used to investigate the hemodynamics of aortic valves, calcium deposition on leaflets and optimization of the design of tissue-engineered heart valves. However, no model currently exists to highlight the distinct mechanical properties of the fibrosa and ventricularis sides of the leaflets, which is critical for proper function of aortic valves. In this study, we developed a FE model with layered structure and realistic distribution of collagen fibers on both sides. The mechanical properties of the two sides were calibrated based on published biaxial testing results, and the effects of alignment of collagen fibers on strain patterns under stretch were also investigated. To mimic the anisotropic and heterogeneous extracellular matrix (ECM) structure of aortic valve leaflets, our model has two layers of hyperelastic matrix with attached collagen fibers on fibrosa and ventriculatis sides. The shapes of the leaflets and the collagen bundle patterns on fibrosa side were adopted from a report by Stella et al. on native porcine aortic valves[1], and the 3D geometric models were developed in Autodesk Inventor. The nonlinear simulation was done in Autodesk Simulation Mechanical environment, and the leaflets were meshed with 3D hexahedral elements to mimic the elastic matrix. In contrast, on ventricularis side, 1D beam elements were added uniformly along the circumferential direction to mimic the thin collagen fibers. Two hyperelastic materials were assigned to elements representing elastic matrix and collagen, and their properties were

described in nonlinear strain-energy functions. This model was tested under biaxial stretch conditions (0% to 25% elongation rates along radial and circumferential directions), and the stress-strain curves of the two separate layers and the entire leaflets were calibrated based on experimental data[2]. The strain patterns were also compared to our digital image correlation (DIC) results. With fewer collagen fibers, the ventricularis side was approximately half as stiff as the fibrosa in the circumferential direction. However, stiffness was similar in the radial direction in both layers. Similar to our DIC results, the simulation results showed that the strain fields retained distinct patterns under different levels of stretch, were anisotropic and reflected features of the collagen bundles. The collagen bundles were the main load bearing component, and the area between them had larger strain. The strain fields on fibrosa side were also more heterogeneous compared to ventricularis due to their ECM distribution (thicker collagen bundles in fibrosa vs. heavy elastic matrix in ventricularis). Using the layered heterogeneous structure, our FE model could reflect the distinct mechanical properties of fibrosa and ventricularis sides of aortic valve leaflets.

Introduction and literature review

Application of finite element method in aortic valve study

The aortic valve serves as a check valve to ensure blood flow direction from the left ventricle into the aorta. The normal valve has three leaflets, controlled by

pressure gradients, which present negligible outflow resistance when open during cardiac ejection and close without leak during ventricular filling to maintain diastolic pressure in the aorta and systemic circulation.[12] Biomedical engineers have long sought to understand and to explain the function of the aortic valve system using computer models. The biomechanics of the aortic valve has been the subject of rigorous study, motivated by the hope that a better understanding of normal valve function will increase understanding of valve disease progression and lead to improved prosthetic valves and to more reliable methods for valve surgical repair. Finite-element models have revealed important information about stress patterns in the valve leaflets, as well as potential valve failure mechanisms.[12] Fluid-structure interaction models for organ-scale heart valve motion have been developed[28], allowing simultaneous prediction of the solid and fluid phases in the valve. In 2008, Kaazempur Mofrad reported development of numerical simulations of heart valves over three range of length scales: organ, tissue and cell levels.[28] Patients with bicuspid aortic valve (BAV) are more likely to develop a calcific aortic stenosis (CAS), as a number of other ailments, as compared to their cohorts with normal tricuspid aortic valves (TAV). It is important to know whether the increase in risk of CAS is caused by the geometric differences between the tricuspid and bicuspid valves or whether the increase in risk is caused by the same underlying factors that produce the geometric difference. Simulations showed that compared to the differences in the tissue and cell level, differences between the tricuspid and bicuspid valves at the organ scale played a more important role: the bicuspid valve

shows greater flexure in the solid phase and stronger jet formation in the fluid phase relative to the tricuspid. This effect appears to play an important role in normal valve function and may have important implications for the design of prosthetic and tissue engineered replacement valves.[28]

For aortic valve replacement surgery, bioprosthetic valves have been increasingly interested since they more resemble the components and structure of native valves, thus result in much less blood clotting.[27] However, they are less durable and also face some common complications such as valve tissue degradation and calcification. Therefore, simulation of the implantation prior to the intervention is an effective and efficient method to optimize the design of bioprosthetic valves. For example, aortic valve reconstruction using leaflet grafts made from autologous pericardium is an effective surgical treatment for some forms of aortic regurgitation. Despite favorable outcomes in the hands of skilled surgeons, the procedure is underutilized because of the difficulty of sizing grafts to effectively seal with the native leaflets. Difficulty is largely due to the complex geometry and function of the valve and the lower distensibility of the graft material relative to native leaflet tissue. Howe et al. used a structural finite element model to explore how a pericardial leaflet graft of various sizes interacts with two native leaflets when the valve is closed and loaded.[9]

In addition, all commercially available porcine valves are pretreated with glutaraldehyde before human implantation, causing inevitable alterations to their mechanical properties. The thickness distribution is also different. In addition, in stented valves, the root is noncompliant. To evaluate the consequences of such treatment on valve mechanics, the opening mechanics of porcine valve substitutes and those of a normal human aortic valve were compared. The opening mechanics of the aortic valve, especially the time taken to open fully from a closed position, and the duration for which the valve is maximally open, were compared in a normal aortic valve, a stent-mounted porcine, and a stentless porcine valve, using a finite element model. Despite a 4-fold higher gradient, stent-mounted porcine valves were slower in attaining the fully open position, and the time for which the valve was fully open was almost 25% less than a normal valve. In stentless valves, the compliant root made the initial opening mechanics similar to those of a normal valve. Once this effect was over, the effect of porcine leaflet properties took over, and there was a corresponding delay in the valve opening. This study suggested that fixing the root with a stent and stiffening the leaflets with glutaraldehyde result in delayed valve opening and decrease the duration for which the valve is fully open, thus contributing to inferior hemodynamics.[25]

Difficulties in simulation of aortic valves

A healthy valve opens and closes competently over billions of cycles and a wide range of heart rates and blood pressures. This durability is attributed to the heterogeneous, layered arrangement of structural proteins and proteoglycans in

the leaflets, with a hierarchical network of collagen fibers believed to bear most of the stress during loading.[22] However, in addition to its stress-bearing role, such a fiber network has the potential to produce functionally important shape changes in the closed valve under pressure load. For example, Nido et al. measured the average pattern of the collagen network in porcine aortic valve leaflets after staining for collagen. They then used finite element simulation to explore how this collagen pattern influences the shape of the closed valve, and observed a curved or bent pattern, with collagen fibers angled downward from the commissures toward the center of the leaflet to form a pattern that is concave toward the leaflet free edge. Simulations showed that these curved fiber trajectories straighten under pressure load, leading to functionally important changes in closed valve shape. Relative to a pattern of straight collagen fibers running parallel to the leaflet free edge, the concave pattern of curved fibers produces a closed valve with a 40% increase in central leaflet coaptation height and with decreased leaflet billow, resulting in a more physiological closed valve shape.[10]

The fluid-structure interaction depends on the solid mechanics of the leaflets, which can be characterized by their stress-strain relationships. Stress is an important biomechanical signal in a variety of tissues. In valve tissue, increased stress has been associated with calcification in bioprosthetic leaflets, and pathological remodeling, each of which is dependent on the direction and magnitude of mechanical stress.[18] Aortic valve leaflets exhibit large deformations

and demonstrate significant anisotropic behavior under equibiaxial loading with stiffer response along the circumferential direction. Several constitutive models have been proposed for the aortic valve. For example, to computationally model the aortic valve tissue, Guccione et al proposed an anisotropic modified Fung-type hyperelastic strain energy function, which was utilized to characterize the aortic valve.[19] There have been numerous experimental, theoretical, and computational studies on the material properties of cardiac tissue. The geometric nonlinearity in the stress-displacement relation based on the finite strain theory produces substantial analytical complications and consequently convergence issues in numerical models. In addition, the large displacement of the leaflets makes the numerical model of the aortic valve complex and challenging for stability, and incorporating the nonlinear property to the cardiac tissue introduces more complexity instability issues to the model. As a result, most of the numerical studies conveyed in the aortic valve area either have studied a small region of the root with more complex material properties or have constructed more developed physiological geometry with simplified linear isotropic material properties.[8]At the tissue scale, many efforts have been made recently to formulate and implement appropriate experimentally-derived material constitutive models. [14, 22, 24]

In addition to this nonlinearity, hyperelasticity and anisotropy, it is well known that the heart valves are heterogeneous structures. The aortic valve cusps, or leaflets, are composed of three layers of tissue: the fibrosa on the aortic side, the

ventricularis on the left ventricle side, and the spongiosa that lie between them. Most of the collagen fibers are aligned in the fibrosa, but they are also embedded in an elastin matrix in the ventricularis layer. The load-bearing functionality of human aortic tissue is mainly determined by elastic lamina, collagen bundles, and smooth muscle cells, and the contribution of smooth muscle cells is known to be insignificant in passive mechanical responses.[19] It is widely assumed that the fibers are oriented principally in the circumferential direction, and therefore, the cusp is more compliant and weaker in the radial direction. However, the orientation of the collagen fibers and their bundle sizes vary inside the cusps.[15, 16] Each valve cusp has its own distinctive fiber alignment with varying orientations and sizes of its fiber bundles. However, little prior mechanical behavior models have been able to account for the valve-specific collagen fiber networks (CFN) or for their differences between the cusps.

Many experimental studies have investigated cusp tissue, and several of them have mapped the orientation and concentration of the collagen fibers. Tower et al. measured the fiber alignment during mechanical testing using polarized light microscopy.[13] Robinson et al. investigated the alignment of the fibers in native and bioartificial valves.[20] Nevertheless, these fiber alignments were not employed in the material models of previous biomechanical simulations. Few numerical studies assumed linear elastic and isotropic or anisotropic tissue behavior. More advanced material models included nonlinear tissue behavior and constitutive models to

account for their complex collagenous structure. Sun and Sacks employed Fung's model for soft tissue, where hyperelasticity was assumed and the Green stress tensor modified.[11, 14, 17] These groups also proposed a method to use Fung's model with biaxial experimental data for a bioprosthetic valve. Kim modeled cusp tissue by modifying Holzapfel's constitutive model that was originally suggested for anisotropic-homogenous arterial tissue.[11] This model was compared with two other models, one included different layers of elements for the collagen fiber network.[7, 15] Some models of the aortic valve have incorporated regional variations within leaflets in order to represent the actual fibrous and layered leaflet structure.[3] De Hart et al. and Driessen et al. modeled the cusps as a fiber-reinforced composite by adjusting the Cauchy stress tensor and adapting the local orientation and magnitude of the principal stretches.[4, 6, 23] However, these orientations were calculated from the deformation tensor and were not based on the experimental results. Only a few numerical models investigated the asymmetry of aortic valves, most of them examining the congenital bicuspid valves. Grande et al. examined the effect of asymmetric patient-specific morphology from magnetic resonance imaging (MRI).[21, 26] However, the material model was simplified anisotropiclinear elastic and did not take into account the asymmetric fiber alignment. The regions with a less dense fiber network are more prone to damage since they are subjected to higher principal stress in the tissues and a higher level of flow shear stress. This asymmetric flow leeward of the valve might damage not only the valve itself but also the ascending aorta. While the modeling of symmetric leaflets greatly

simplifies the finite-element analysis, this assumption may not be justified by the actual anatomy of normal valves, and may limit the accuracy of the model findings. Differences in the shape and size of the three aortic valve leaflets: right, left, and non-coronary have been widely recognized, although infrequently incorporated into computational valve analyses.

In summary, while an ideal structural model for aortic leaflets need to be anisotropic, nonlinear and heterogeneous, there is no prior studies that could simulation their behaviors accurately. Our previous studies showed that the distinct structures and strain patterns between fibrosa and ventricularis play critical roles in the proper function of aortic valves. Therefore we designed a layered finite element model with realistic distribution of collagen fibers on both sides to improve accuracy of simulation.

Method

We aim to develop a FE model that can better mimic the nonlinear, anisotropic and heterogeneous mechanical properties of native aortic leaflets. Our model will be based on three main criteria: 1) correspond to the nonlinear over all stress-strain relationship of native aortic leaflets; 2) have multi-layered structure with varied thickness to mimic the fibrosa and ventricularis respectively; 3) have similar strain pattern to the DIC results under biaxial stretch.

Simulation will be applied in Autodesk Simulation Mechanical since it includes Autodesk Nastran FEA (finite element analysis) solver software, and provides tools for FEA and modeling, which enables more complex meshing compared to custom FEA codes. Nastran is a FORTRAN based software and allows manual modification of input cards in which analysis type, elements, material properties and loads/constrains are defined. Autodesk Nastran features multiple build-in hyperelastic and anisotropic materials, and can automatically create contact pairs between two parts when conducting contact analysis.

Geometric model

An accurate geometric model of aortic valve is necessary for a successful simulation. Current in-vivo methods for geometrical representations of the aortic vales use limited echocardiographic measurements often in two-dimensional sections. The complex three-dimensional geometry of the native tricuspid aortic valve is represented by select parametric curves allowing for a general construction and representation of the 3D structure including the cusps, commissures and sinuses. For example, Raanani et al. used a general mathematical description performed based on three independent parametric curves, two for the cusp and one for the sinuses. These curves are used to generate different surfaces that form the structure of the AV.[7, 8] A similar non-invasive approach method could also been used to measure surface strain and deformations of leaflets: both functional and residual in semilunar valves and apply it to normal human valve leaflets. Transesophageal 3D echocardiographic images

were acquired from open-heart transplant patients, with each leaflet excised after heart explant and then imaged in a flattened configuration ex-vivo. Using an established spline parameterization of both 3D Esegmentations and digitized ex-vivo images, surface strains were calculated for deformation.[2]

However, the use of homografts to obtain the geometry was preferred over the use of in vivo human aortic roots because the ex vivo homograft specimens could be imaged at greater resolution and could be fixed in an unpressurized, zero-load state. The model development was accomplished in four steps: 1) fixing the specimens in unpressurized states using silicone rubber; 2) magnetic-resonance imaging; 3) processing of the resulting images to extract three dimensional data coordinates; and 4) assembly of data coordinates, material properties, thicknesses, and boundary and loading conditions into the final computational model. 3D model could also be built from leaflets and then assemble them to include the aligned collagen fibers in the native leaflets. Haj-Ali et al. tested the effect of collagen bundle orientation on the loaded valve using a structural finite element model.[1] Average leaflet shape and collagen bundle orientation in the model are measured from the porcine valves. The cusps were preserved in a 3% formaldehyde solution for four to five days. After achieving transparent tissue with observable fiber bundles. The bundle alignments were measured from three cusps of a single valve while being fixed in a stretched state. Then, based on the published observation that the aortic valve leaflet attachment lies on a cylinder[15],

the planar leaflet meshes are connected at the free edge termini and wrapped into a cylinder. In our study, the shape of the leaflet were adopted from a native porcine aortic leaflet that is available from a published work[24]. Polarized light images have been used to investigate the collagen bundle alignment in fibrosa. As shown in Figure 17, fiber bundles appear yellow-orange and membranes appear blue as a result of the use of transmitted elliptically polarized light imaging. Overall, fiber bundles appeared to present a cross-hatched, overlapping structure with thin connecting membranes. Traces of the major fiber bundles (right) clarified primary structures of the leaflet. It has been reported that the thickness of the elastic fiber network in the spongiosa is significantly thicker in the hinge and coaptation region than in the belly region of the aortic valve leaflet.

Sacks et al. studied the distinct mechanical properties of fibrosa and ventricularis by separating aortic leaflets from the spongiosa and calculating the stress-strain curves of two layers under biaxial stretch.[17] Comparisons between the fibrosa and ventricularis indicate that the fibrosa side has a greater elastic modulus in the circumferential direction but a similar elastic modulus in the radial direction. These mechanical differences are largely the result of the number of aligned collagen fibers in each direction. With fewer collagen fibers, the ventricularis side is approximately half as stiff as the fibrosa in the circumferential direction. In the radial direction, however, each layer contains approximately the same amount of collagen fibers and has similar elastic Moduli. Therefore, it’s reasonable to use a

double-layered mesh to mimic the fibrosa and ventricularis sides mentioned above. Rami Haj-Ali et al. has reported a single layer anisotropic and heterogeneous FE model in which collagen bundles embed in an elastin matrix.[1] While two isotropic hyperelastic materials were assigned to these elements, anisotropy and heterogeneity was achieve by aligning the collagen bundles. We used a similar scheme to assign the material properties. The parameters of the material properties and collagen fiber dimensions were optimized to correspond to the experimental data of fresh aortic leaflet tissues. Instead of using a continuum model, though, we took a discrete approach. The solid mesh elements were modeled with an isotropic material. One-dimensional cable elements were then used to connect the nodes of the solid element. The leaflets were 3D modeled in Autodesk Inventor, then be meshed in Simulation Mechanical with two layers of hexahedral elements across the thickness. Fig. 20 shows a top view of the mesh. 1D beam elements will be manually added on the two surfaces of the mesh to mimic collagen bundles (Fig. 21). On the fibrosa side, collagen network with thick bundles shown in figure 17 will be applied; while on the ventricularis side, uniform thin fibers will be aligned along circumferential direction in each 3D element. Ventri collagen alignment, decellularized valve design.

Hyperelastic material models

For describing the behaviors of inear anisotropic materials under stretch conditions, only nine constants will be enough, including Ecirc: elastic modulus in the circumferential direction; Elong: elastic modulus in the longitudinal direction;

Erad: elastic modulus in the radial direction; Gxy: shear modulus in the xy plane; Gxz: shear modulus in the xz plane; Gyz: shear modulus in the yz plane; n: Poisson's ratio.[5] However, for describing the stress-strain relationships of hyperelastic materials, strain energy densities have to be used. Various hyperelastic material models have been developed based on invariants deformation for strain density functions, among which Mooney-Rivlin models and Ogden material model have been widely used in simulation of rubber-like materials. In our study, we tested the 2-constant standard form and 5-constant high-order form of Mooney-Rivlin models as well as third and fifth-order Ogden model to investigate how these material models would affect the curve fitting of experimental data, and try to optimize the material constants for the simulation. The material constants were identified using the Levenberg-Marquardt nonlinear regression method such that the fitted response matched the experimental data with correlation coefficients greater than 0.99. For material models with higher orders, least-squire method was used to search for optimized material constants in a larger potential ranges when the Levenberg-Marquardt nonlinear regression method could not generate data with enough precision.

2-constant standard Mooney-Rivlin model:

$$W = C_{10}(\overline{I_1} - 3) + C_{01}(\overline{I_2} - 3) + \sum_{i=1}^{N} \frac{\mathrm{K_i}}{2}(\mathrm{J_3} - 1)^{2i}$$

5-constant high-order Mooney-Rivlin model:

$$W = C_{10}(\overline{I_1} - 3) + C_{01}(\overline{I_2} - 3) + C_{20}(\overline{I_1} - 3)^2 + C_{11}(\overline{I_1} - 3)(\overline{I_2} - 3) + C_{02}(\overline{I_2} - 3)^2 + \sum_{i=1}^{N} \frac{K_i}{2}(J_3 - 1)^{2i}$$

Cij are material constants, J3 is the determinant of the strain gradient tensor, Ki is a material constant related to the bulk modulus

Ogden material model:

$$W = \sum_{i=1}^{N} \frac{\mu_i}{\alpha_i}\left(\overline{\lambda_1^{\alpha_i}} + \overline{\lambda_2^{\alpha_i}} + \overline{\lambda_3^{\alpha_i}} - 3\right) + \sum_{i=1}^{N} \frac{K_i}{2}(J_3 - 1)^{2i}$$

μi, αi are material constants, J3 is the determinant of the strain gradient tensor, Ki is a material constant related to the bulk modulus.

Results and Discussion

Based on Sacks et al.'s report, the thickness of the entire leaflets was set to be 0.55mm, while the thicknesses of fibrosa and ventriculairs sides were 0.35mm and 0.2mm, respectively. The 3D model of the whole leaflets were developed in Autodesk Inventor first, then was trimmed to be rectangular as in our previous study with dimensions of 20mm X 16mm. To test the various hyperelastic material models and optimize the material constant, finite element model of a specimen located near the root area of the ventricularis side was built with dimensions of 4mm X 4mm. As shown in Fig. 22, our finite element model showed anisotropic and hyperelastic stress-strain relationships. In the circumferential direction, the

stiffness of tissue was larger since on ventricularis side, collagen fibers, the major load bearing component in the extracellular matrix, mostly aligned along this direction. Also in this direction, all four hyperelastic material models could generate fitted curves with good precision, and the Mooney-Rivlin model with 5 constants generated the most accurate results. However, in the radial direction, in which the stretch ratio could be greater than 25%, only the material models with higher orders could generate curves that replicate the experimental data. Also the 5-constant high-order Mooney-Rivlin model and the fifth-order Ogden material model could both fulfill the requirement, we chose the Mooney-Rivlin model for simulation of the entire leaflet, since it was more time-cost efficient and the results were more stable when testing multiple sets of experimental data using various stretch schemes such as uniaxial strip stretch and biaxial stretch.

Various biaxial stretch conditions were tested on the entire leaflets, along radial direction stretch ratio of 0%, 5%, 15% and 25% were used, while along circumferential direction, stretch ratio were set to be 0%, 5%, 10%, 15% in combination of the stretch along radial direction. We also compared the strain patterns on the fibrosa and ventricularis sides of the leaflets generated by the simulation to our previous digital image correlation results, and the simulation could well replicate the experimental results, showing the distinct features of collagen bundle/fiber alignment though the strain distribution. As shown in Figure 23 and 24, strain along radial direction showed more features of ECM structure

since the thick collagen bundles and thin collagen fibers align mostly along the circumferential direction. Thus during stretch, the areas between the thick collagen bundles deformed first and experienced largest strains. Strain on ventricularis sides were more even than fibrosa sides. This is because the loading bearing collagen bundles locate on the fibrosa sides, while on the venricularis side, thin collagen fibers distributes more evenly, and they function with elastic fibers to responsible for both recoil and integrity of the leaflets. Unlike the right and coronary leaflets, the strain fields on the left leaflets were asymmetric, which reflected the unique distribution of aollagen bundles in the left leaflet.

For the entire leaflet under equibiaxial stretch, the finite elemnent model could well replicate the stress-strain relationship along the circumferential direction when the stress was under 50000 N/m^2, as shown in Figure 25. While the stress was increasing further, the experimental data showed that the stretch ratio was decreasing slightly, which was induced by effects of relatively large Poisson ratio when the stress of the sample along circumferential direction was increased simultaneously. However, the simulation results did not showed this effect, which suggested that the constant of the materials regarding Poisson ratio needed to be modified. In addition, along the radial direction, the simulation resulted a curve that had a lower gradient near the stretch ratio of 1.4. In native tissues, the hyperelasticity shows a nearly bi-linear stress-strain curve, with a dramatic gradient change near this stretch ratio. It has been a common limitation in

simulation of aortic valve tissues. In future, custom codes for optimization of material constants need to be developed to improve the accuracy of stress-strain curves of entire leaflets under equibiaxial stretch conditions.

Conclusion

Using a bi-layer design, our finite element model used 3D brick elements to mimic the elastic matrix, and used 1D beam element to mimic the distinct distributions of thick collagen bundles and thin collagen fibers on the fibrosa and ventricularis sides of aortic valve leaflets. Similar to our experimental results, the simulation results showed that the strain fields retained distinct patterns under different levels of stretch, were anisotropic and reflected features of the collagen bundles. The strain fields on fibrosa side were also more heterogeneous compared to ventricularis due to their ECM distribution (thicker collagen bundles in fibrosa vs. heavy elastic matrix in ventricularis). Using the layered heterogeneous structure, our FE model could reflect the distinct mechanical properties of fibrosa and ventricularis sides of aortic valve leaflets.

References

1. Marom G, Peleg M, Halevi R, Rosenfeld M, Raanani E, Hamdan A and Haj-Ali R. Fluid-structure interaction model of aortic valve with porcine-specific collagen fiber alignment in the cusps. *J Biomech Eng.* 135:101001-101006, 2013.
2. Aggarwal A., A. M. Pouch, E. Lai, J. Lesicko, P. A. Yushkevich, J. H. Gorman Iii, R. C. Gorman and M. S. Sacks. In-vivo heterogeneous functional and residual strains in human aortic valve leaflets. *J Biomech* 49: 2481-2490, 2016.
3. Anssari-Benam A., A. H. Barber and A. Bucchi. Evaluation of bioprosthetic heart valve failure using a matrix-fibril shear stress transfer approach. *J Mater Sci Mater Med* 27: 42, 2016.
4. Boerboom R. A., N. J. B. Driessen, C. V. C. Bouten, J. M. Huyghe and F. P. T. Baaijens. Finite Element Model of Mechanically Induced Collagen Fiber Synthesis and Degradation in the Aortic Valve. *Annals of Biomedical Engineering* 31: 1040-1053, 2003.
5. Buchanan R. M. and M. S. Sacks. Interlayer micromechanics of the aortic heart valve leaflet. *Biomech Model Mechanobiol* 13: 813-826, 2014.
6. Driessen N. J. B., C. V. C. Bouten and F. P. T. Baaijens. Improved Prediction of the Collagen Fiber Architecture in the Aortic Heart Valve. *Journal of Biomechanical Engineering* 127: 329, 2005.
7. Haj-Ali R., G. Marom, S. Ben Zekry, M. Rosenfeld and E. Raanani. A general three-dimensional parametric geometry of the native aortic valve and root for biomechanical modeling. *J Biomech* 45: 2392-2397, 2012.
8. Halevi R., A. Hamdan, G. Marom, K. Lavon, S. Ben-Zekry, E. Raanani, D. Bluestein and R. Haj-Ali. Fluid-structure interaction modeling of calcific aortic valve disease using patient-specific three-dimensional calcification scans. *Med Biol Eng Comput* 54: 1683-1694, 2016.
9. Hammer P. E., P. C. Chen, P. J. del Nido and R. D. Howe. Computational model of aortic valve surgical repair using grafted pericardium. *J Biomech* 45: 1199-1204, 2012.

10. Hammer P. E., C. A. Pacak, R. D. Howe and P. J. del Nido. Straightening of curved pattern of collagen fibers under load controls aortic valve shape. *J Biomech* 47: 341-346, 2014.

11. Joyce E. M., J. Liao, F. J. Schoen, J. E. Mayer, Jr. and M. S. Sacks. Functional collagen fiber architecture of the pulmonary heart valve cusp. *Ann Thorac Surg* 87: 1240-1249, 2009.

12. K. JANE GRANDE R. P. C., PER G. REINHALL, AND KARYN S. KUNZELMAN†. <0-1-1998-KARYN S. KUNZELMAN- different thickness.pdf>. *Annals of Biomedical Engineering* 26: 534-545, 1998.

13. Lee C. H., R. Amini, R. C. Gorman, J. H. Gorman, 3rd and M. S. Sacks. An inverse modeling approach for stress estimation in mitral valve anterior leaflet valvuloplasty for in-vivo valvular biomaterial assessment. *J Biomech* 47: 2055-2063, 2014.

14. Li K. and W. Sun. Simulated transcatheter aortic valve deformation: A parametric study on the impact of leaflet geometry on valve peak stress. *Int J Numer Method Biomed Eng* 33: 2017.

15. Marom G., R. Haj-Ali, M. Rosenfeld, H. J. Schafers and E. Raanani. Aortic root numeric model: annulus diameter prediction of effective height and coaptation in post-aortic valve repair. *J Thorac Cardiovasc Surg* 145: 406-411 e401, 2013.

16. Marom G., R. Halevi, R. Haj-Ali, M. Rosenfeld, H. J. Schafers and E. Raanani. Numerical model of the aortic root and valve: optimization of graft size and sinotubular junction to annulus ratio. *J Thorac Cardiovasc Surg* 146: 1227-1231, 2013.

17. Martin C. and W. Sun. Biomechanical characterization of aortic valve tissue in humans and common animal models. *J Biomed Mater Res A* 100: 1591-1599, 2012.

18. May-Newman K., C. Lam and F. C. Yin. A hyperelastic constitutive law for aortic valve tissue. *J Biomech Eng* 131: 081009, 2009.

19. Mohammadi H., R. Cartier and R. Mongrain. 3D physiological model of the aortic valve incorporating small coronary arteries. *Int J Numer Method Biomed Eng* 33: 2017.

20. Moreira R., C. Neusser, M. Kruse, S. Mulderrig, F. Wolf, J. Spillner, T. Schmitz-Rode, S. Jockenhoevel and P. Mela. Tissue-Engineered Fibrin-Based Heart Valve with Bio-Inspired Textile Reinforcement. *Adv Healthc Mater* 5: 2113-2121, 2016.

21. Puperi D. S., R. W. O'Connell, Z. E. Punske, Y. Wu, J. L. West and K. J. Grande-Allen. Hyaluronan Hydrogels for a Biomimetic Spongiosa Layer of Tissue Engineered Heart Valve Scaffolds. *Biomacromolecules* 17: 1766-1775, 2016.

22. Sacks M. S. and A. P. Yoganathan. Heart valve function: a biomechanical perspective. *Philos Trans R Soc Lond B Biol Sci* 362: 1369-1391, 2007.

23. Sanders B., S. Loerakker, E. S. Fioretta, D. J. Bax, A. Driessen-Mol, S. P. Hoerstrup and F. P. Baaijens. Improved Geometry of Decellularized Tissue Engineered Heart Valves to Prevent Leaflet Retraction. *Ann Biomed Eng* 44: 1061-1071, 2016.

24. Stella J. A., J. Liao and M. S. Sacks. Time-dependent biaxial mechanical behavior of the aortic heart valve leaflet. *J Biomech* 40: 3169-3177, 2007.

25. Subhani M., R. K. Kumar and K. R. Balakrishnan. Normal aortic valves stay open much longer in systole than porcine substitutes. *Asian Cardiovasc Thorac Ann* 21: 275-280, 2013.

26. Tseng H. and K. J. Grande-Allen. Elastic fibers in the aortic valve spongiosa: a fresh perspective on its structure and role in overall tissue function. *Acta Biomater* 7: 2101-2108, 2011.

27. Votta E., L. Paroni, C. A. Conti, A. Pelosi, A. Mangini, P. D'Alesio, R. Vismara, C. Antona and A. Redaelli. Aortic valve repair via neo-chordae technique: mechanistic insight through numerical modelling. *Ann Biomed Eng* 40: 1039-1051, 2012.

28. Weinberg E. J. and M. R. Kaazempur Mofrad. A multiscale computational comparison of the bicuspid and tricuspid aortic valves in relation to calcific aortic stenosis. *J Biomech* 41: 3482-3487, 2008.

Appendix

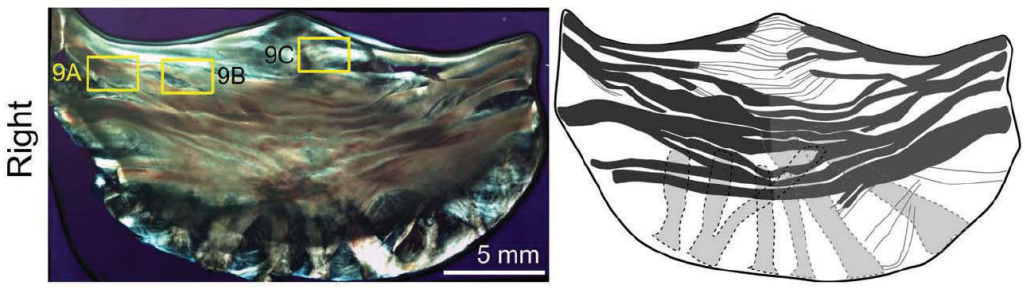


Figure 17. Polarized light image and major fiber bundles of a leaflet

Source: Rock, Christopher A.. Lin Han, Todd C. Doehring. PLoS ONE 9(2014): e86087

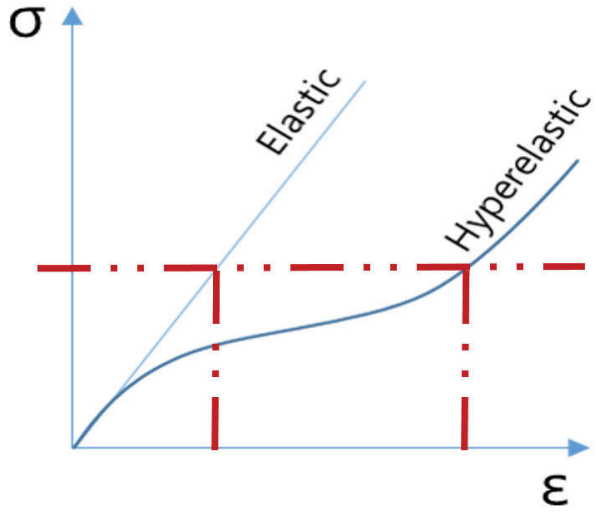


Figure 18. Stress-strain relationships

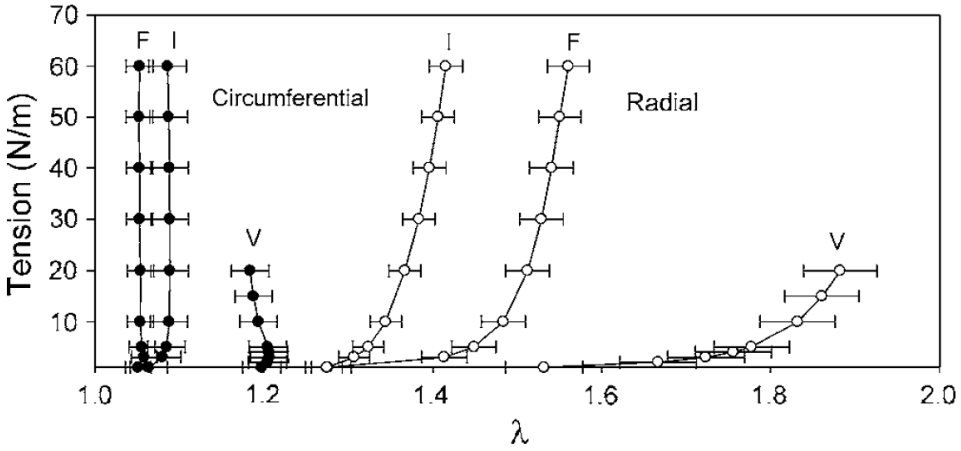


Figure 19. Experimental data on two sides of leaflets

I= Intact leaflets F= Separated Fibrosa side V= Separated Ventricularis side

Source: Stella, John A., and Michael S. Sacks. *Journal of biomechanical engineering*129 (2007): 757-766.

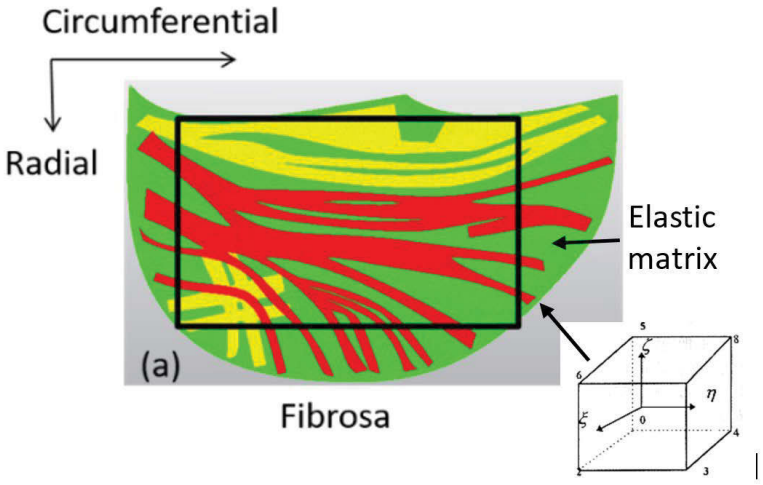


Figure 20. Elastic base was meshed with 3D elements

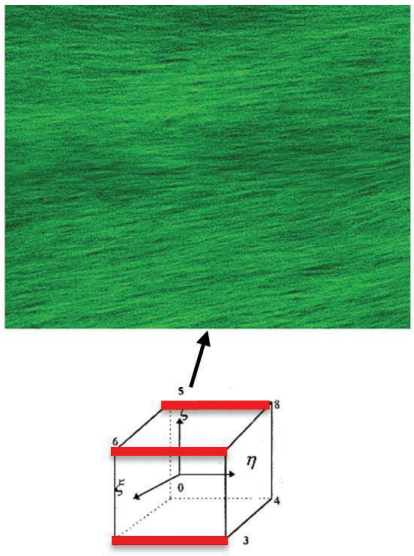


Figure 21. Collagen fibers were meshed with 1D elements

Collagen fibers align circumferentially on ventricularis side. 1D beam elements were added to the 3D elements for elastic base automatically

Source: Sanders B., S. Loerakker, E. S. Fioretta, D. J. Bax, A. Driessen-Mol, S. P. Hoerstrup and F. P. Baaijens. *Ann Biomed Eng* 44: 1061-1071, 2016.

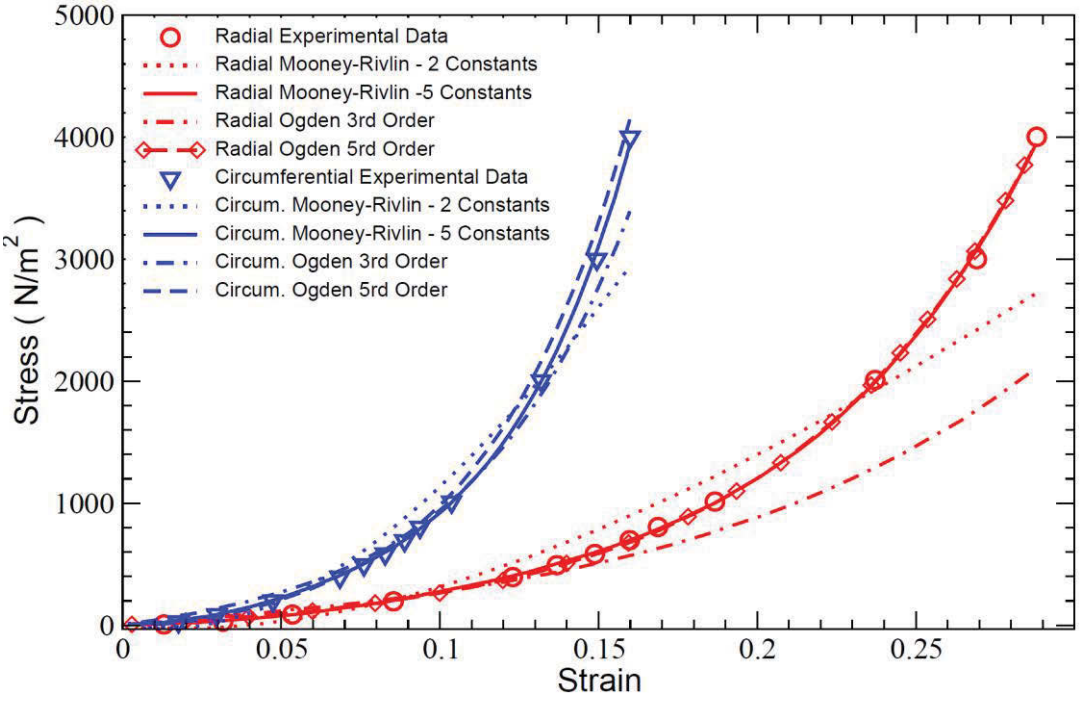


Figure 22. Curve fitted stress-strain relationships under uniaxial stretch

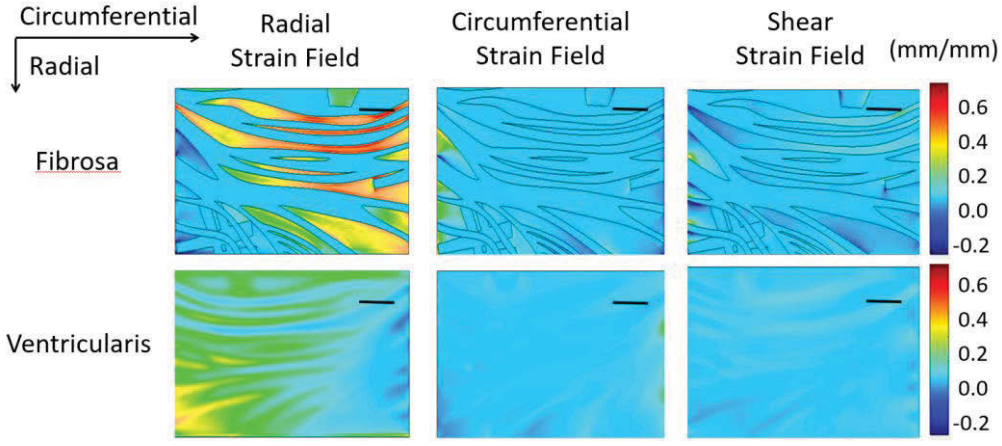


Figure 23. Strain patterns generated by simulation

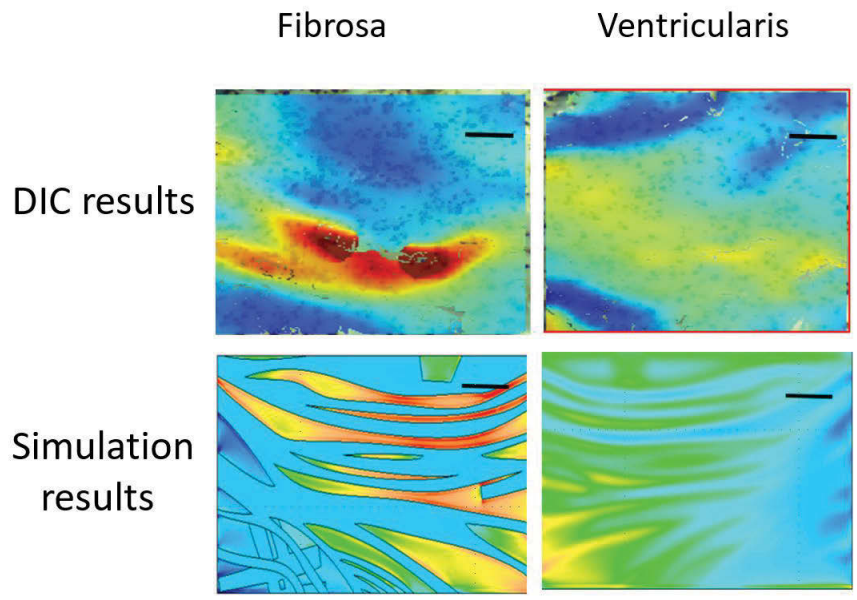


Figure 24. Validation of strain patterns

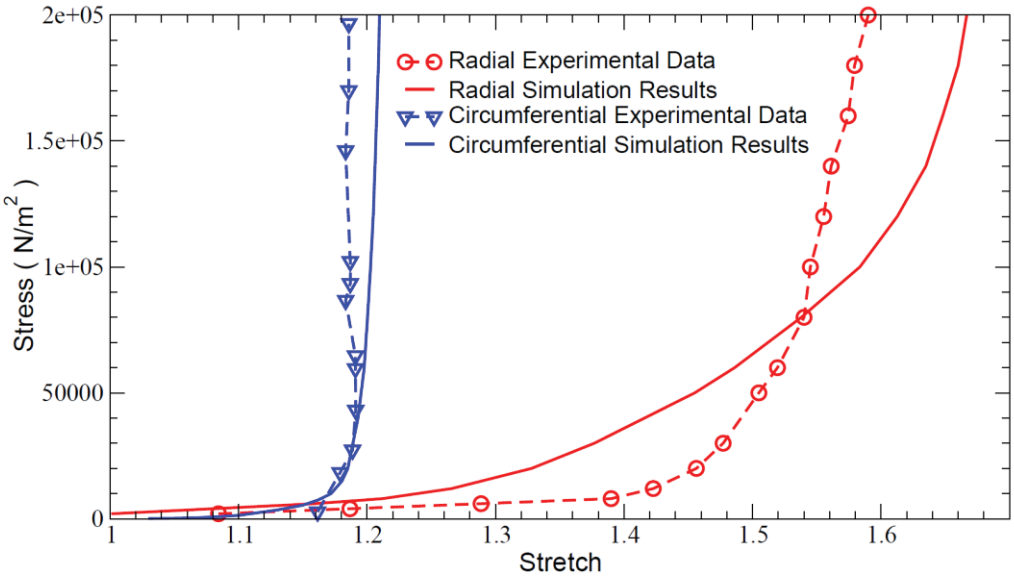


Figure 25. Constitutive model under equibiaxial stretch

CONCLUSION

Cyclic stretch is known to modulate ECM fiber synthesis and alignment. However, little tools are available for studying the interaction between aortic tissues and stretch condition. Finite element method is a powerful tool to simulate the complex structure of aortic valve, however, most current simulations modeled the leaflet as a homogenous material, and none of them took the distinctions between two surface layers into account, which were critical for the proper function of the aortic valve. This dissertation developed novel tools to study the effects of cyclic stretch on extracellular matrix remodeling, the heterogeneous properties of the aortic leaflet and the effects of heterogeneity on the function of valve. Firstly, a biaxial stretch bioreactor that can provide precisely controlled stretch and detailed strain field monitoring was designed and fabricated. Its ability of applying predesigned stretch was validated by a silicone rubber membrane and an aortic leaflet tissue. Their detailed strain fields were tracked to show the feasibility of digital image correlation method. The ability of providing sterile environment during stretch were verified by culturing four aortic leaflet tissues for two weeks. In addition, we measured the strain patterns of freshly isolated coronary vs. noncoronary leaflets and fibrosa vs. ventricularis sides of the leaflets under stretch to gain more insights into the heterogeneity and anisotropy of the native aortic valve. Furthermore, a heterogeneous FE model with reinforced fibers on both fibrosa and ventricularis sides was developed. Optimized hyperelastic properties was assigned to the two

materials to ensure the stress-strain relationship mimicking the native aortic leaflets. The FE model was tested under a biaxial stretch condition to study the effects of parameters of material properties and distribution of collagen fibers on the function of aortic valve.

Our research provided insights into 1) the interaction between aortic valve tissue and the mechanical environment, 2) anisotropy and heterogeneity of aortic leaflets ECM due to the distribution of collagen fibers, and 3) detailed distinct strain patterns in fibrosa vs. ventricularis sides and 3 aortic leaflets. Our novel biaxial stretch bioreactor and refined FE model of aortic leaflet have paved path for other scientists to study mechanobiology, design and condition engineered tissues and facilitated simulation of fluid-structure interaction, calcium deposition, transcatheter aortic valve as well as design of implants for aortic valve replacement or repair.

VITA

Ying Lei earned her Bachelor of Science degree from the Beihang University, or the University of Aeronautics and Astronautics (BUAA) with a major in Aircraft Design. With a solid mechanical background, she was interested in implementing engineering tools to solve biomedical problems. She finished her thesis titled ‘‘A Study of Influence of Osteoporosis on Internal Fixation for Femoral Neck Fractures using Finite Element Method’ with instructions from Dr. Qizhi Wang. She joined Dr. Zhiqiang Wan’s lab in 2009 to pursue her Master’s Degree in Aircraft Design, in which she investigated the aerodynamic-thermal-structural interaction in hypersonic flights, designed the iterative algorithm in Matlab and called commercial codes to calculate the fluid fields and structural deformations. After working as a R&D Engineer in Beijing, China for one and a half years, she started her Ph.D. program under the supervision of Dr. Zannatul Ferdous to study the biomechanics, pathology and mechanobiology of aortic valves in the University of Tennessee, Knoxville. Her current researches focus on bioreactor design, finite element analysis of heart valve leaflets, and investigation of extracellular matrix (ECM) remodeling and porcine aortic valve cell calcification under cyclic biaxial stretch conditions.